Conversion between spin and charge currents by Rashba or Topological Insulator interfaces and perspective for low power spintronic devices

1) Introduction to spin-orbitronics.
2) Conversion between charge and spin current with Rashba or TI Interfaces.
3) Potential of TI for applications

A. Barhélémy, M. Bibes, **A. Fert**, J-M. George, H.Jaffres, E. Lesne, N. Reyren, **J-C Rojas-Sánchez**, **CNRS/Thales, Palaiseau, France**
L. Vila, J.-P. Attané, G. Desfond, Y. Fu, S. Gambarelli, M. Jamet, A. Marty, S. Oyarzun,. L. Vila, **CEA Grenoble, France**
J.M. De Teresa, **Un. Zaragoza**, Y. Ohtsubo, **Osaka University**
P. LeFevre, F. Bertran, A. Taleb, **SOLEIL Synchrotron, Gif, France**
C.Rinaldi, R.Bertacco, **Poli.Milan,** R.Calarco, R.Wang,**Drude Inst. Berlin**

Conversion between spin and charge currents by Rashba or Topological Insulator interfaces at Room Temp. and perspective for low power spintronic devices

1) Introduction to spin-orbitronics.

2) Conversion between charge and spin current with Rashba or TI Interfaces.

3) **Potential of TI for applications**

A. Barhélémy, M. Bibes, **A. Fert**, J-M. George, H.Jaffres, E. Lesne, N. Reyren, **J-C Rojas-Sánchez**, **CNRS/Thales, Palaiseau, France**
L. Vila, J.-P. Attané, G. Desfond, Y. Fu, S. Gambarelli, M. Jamet, A. Marty, S. Oyarzun,. L. Vila, **CEA Grenoble, France**
J.M. De Teresa, **Un. Zaragoza**, Y. Ohtsubo, **Osaka University**
P. LeFevre, F. Bertran, A. Taleb, **SOLEIL Synchrotron, Gif, France**
C.Rinaldi, R.Bertacco, **Poli.Milan,** R.Calarco, R.Wang,**Drude Inst. Berlin**

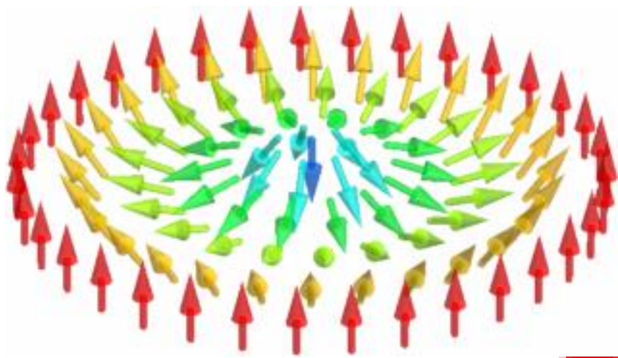

2D
Interface- induced skyrmions and chiral domain walls

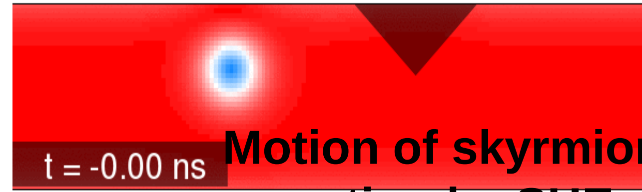

Motion of skyrmion motion by SHE

2D
Graphene + spin-orbit

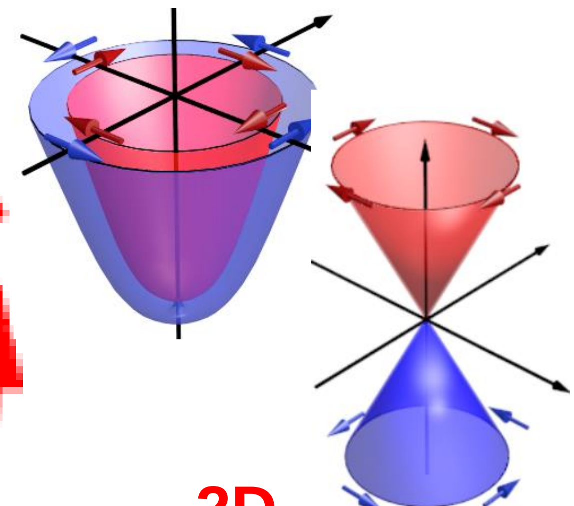

Spin-orbitronics

3D
Spin Hall effect

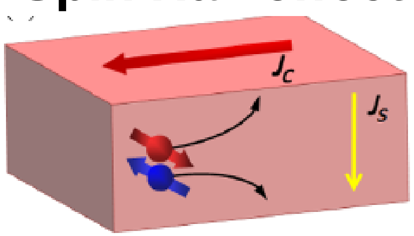

2D
Edelstein-type effects at Rashba and topological insulator interfaces

2D
Oxide interfaces

CNRS · THALES · Université Paris-Sud 11 · CEA

Bulk materials

3D charge current → 3D spin current conversion by Spin Hall Effect (SHE) and 3D spin current → 3D charge current by Inverse SHE (ISHE)

J_S = vertical spin current injected into an adjacent layer by SHE

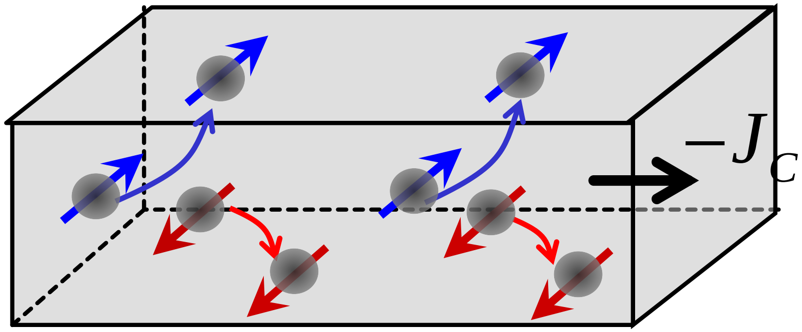

Switching of nanomagnet by the spin current J_S injected by the SHE in an adjacent SO layer

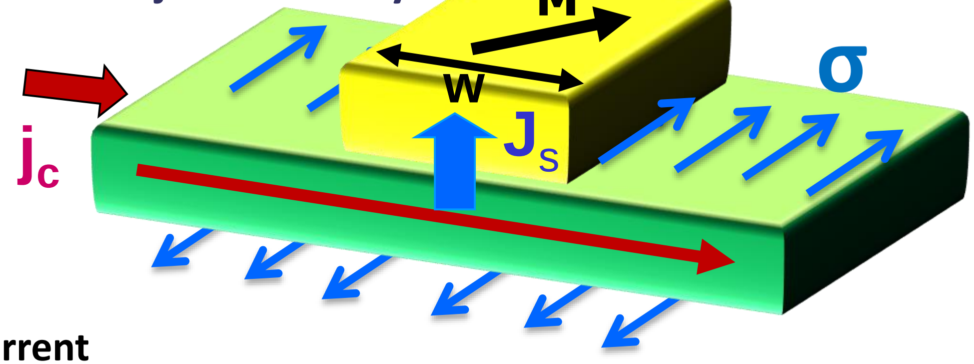

➔ Yield of conversion between charge and spin current

Spin hall angle $\theta_{SHE} = \frac{spin\ current\ density}{charge\ current\ density}$ **(dimensionless)**

Bulk materials

3D charge current → 3D spin current conversion by Spin Hall Effect (SHE) and 3D spin current → 3D charge current by Inverse SHE (ISHE)

J_S = vertical spin current injected into an adjacent layer by SHE

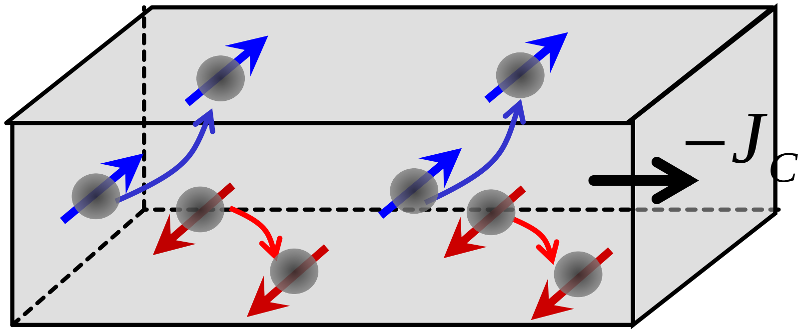

Switching of nanomagnet by the spin current J_S injected by the SHE in an adjacent SO layer

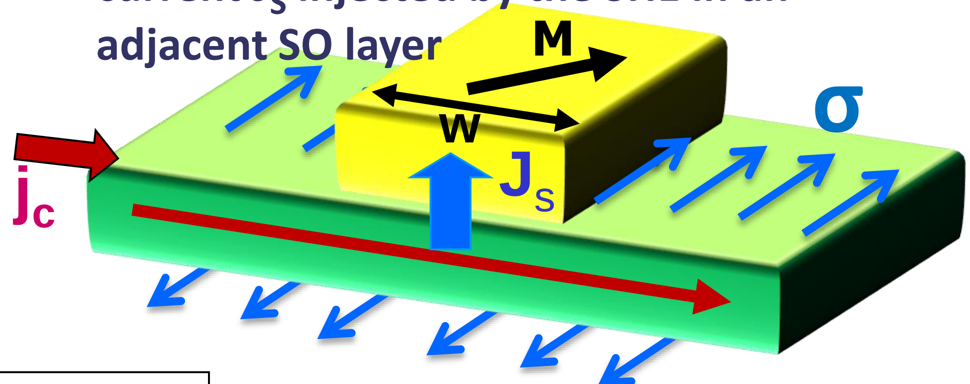

3-terminal SOT-MRAM

M.Cubukcu et al., APL 2015 : switching in 0.4ns current pulse ≃ 10^8 Amp/cm^2 in 1kOe

Z. Wang, W. S. Zhao et al., J. Phys. D 2015 : STT + SOT < 1ns, zero field, current densities ≃ 10^7 Amp/cm^2

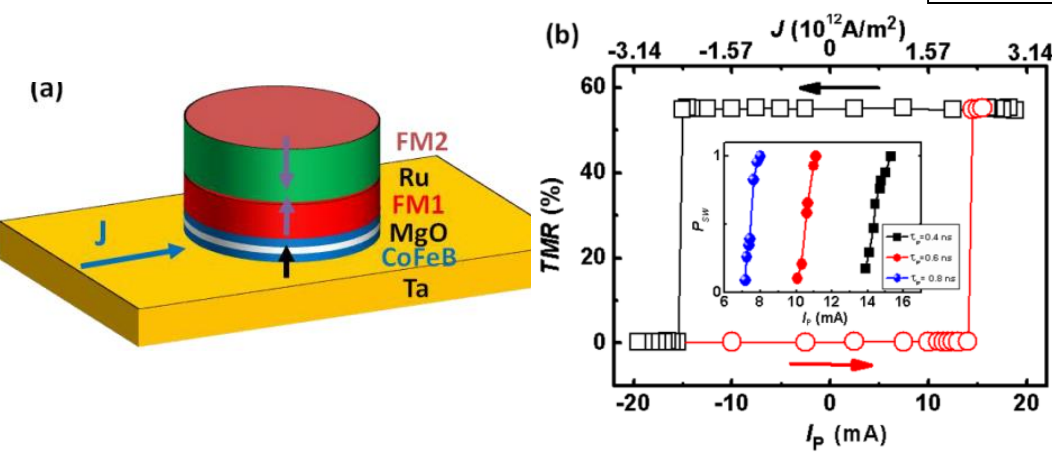

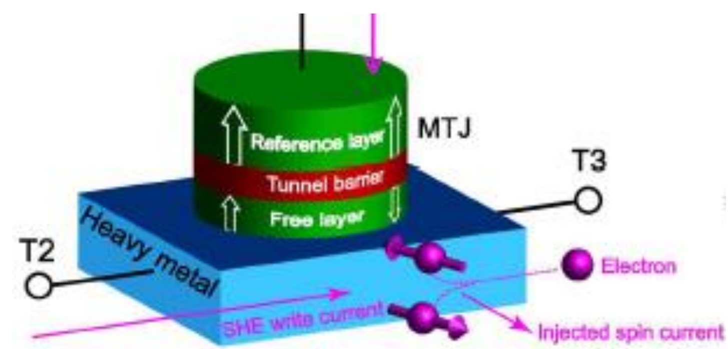

Spin/charge conversion by Rashba interfaces and topological insulators

Rashba interface

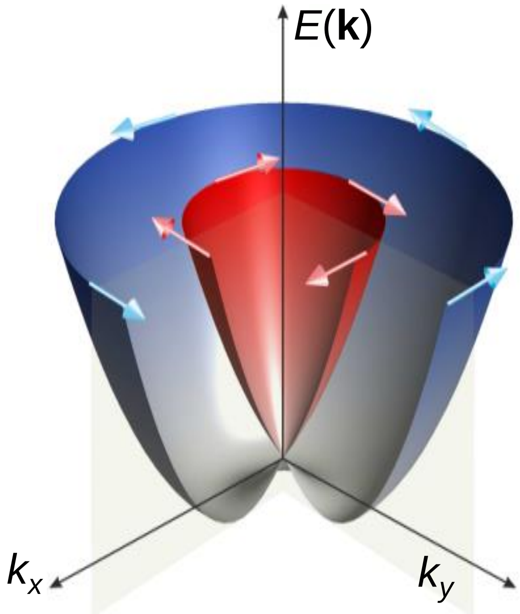

$$\hat{H}_{SO} = \alpha_R \boldsymbol{\sigma} \cdot (\mathbf{k}_{\parallel} \times \mathbf{e}_z),$$

α_R = Rashba coefficient
(example at the Bi/Ag interface 2DEG)

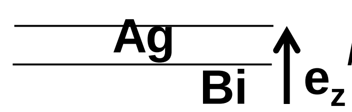

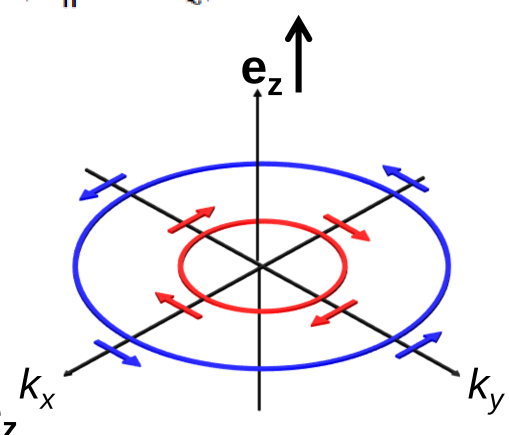

Topological insulator

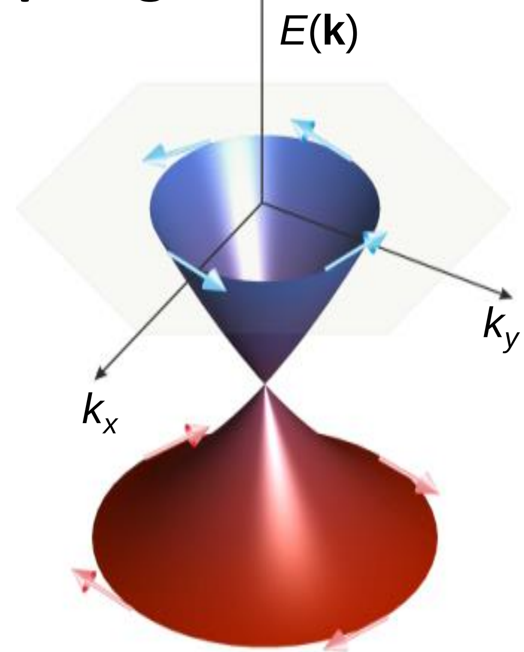

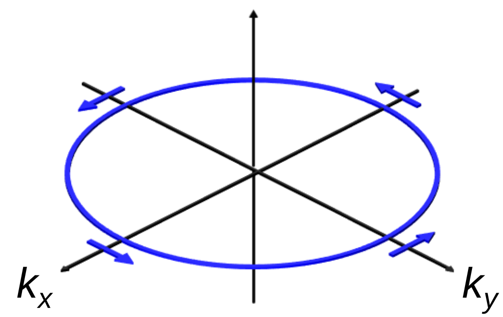

Spin/charge conversion by Rashba interfaces and topological insulators

Rashba interface

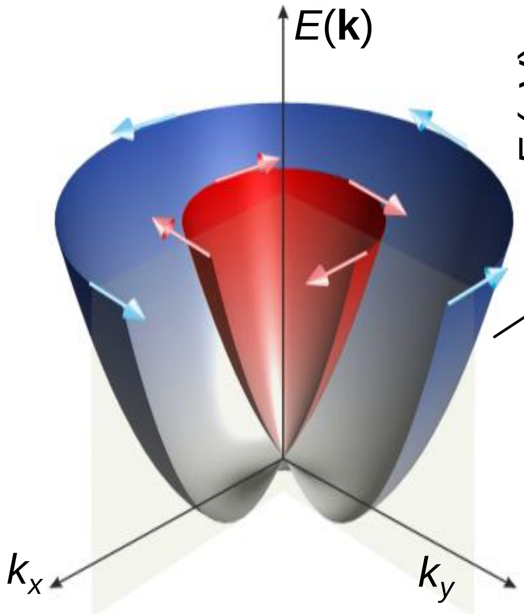

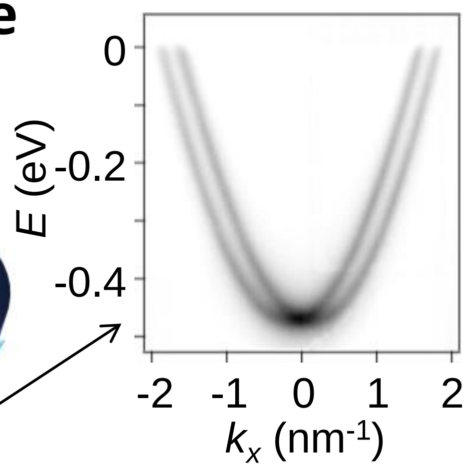

$$\hat{H}_{SO} = \alpha_R \boldsymbol{\sigma}\cdot(\mathbf{k}_{\parallel}\times\mathbf{e}_z),$$

α_R = Rashba coefficient
(example at the Bi/Ag interface 2DEG)

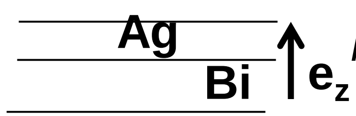

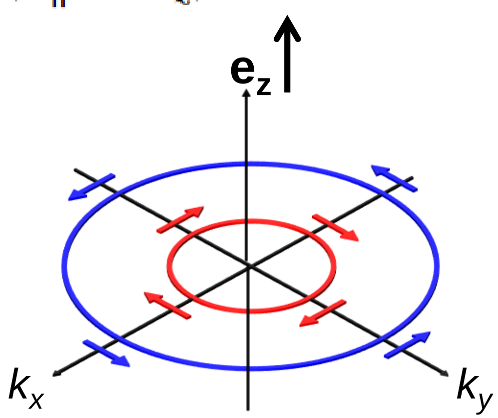

Topological insulator

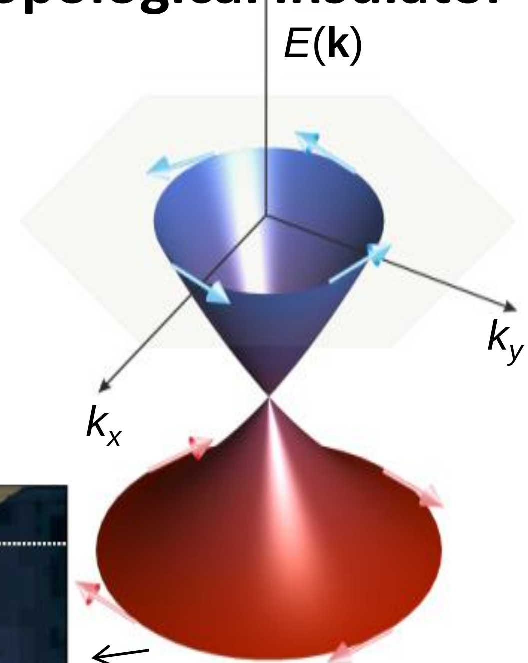

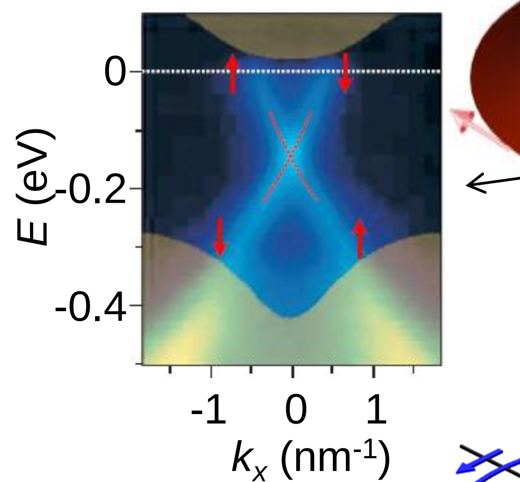

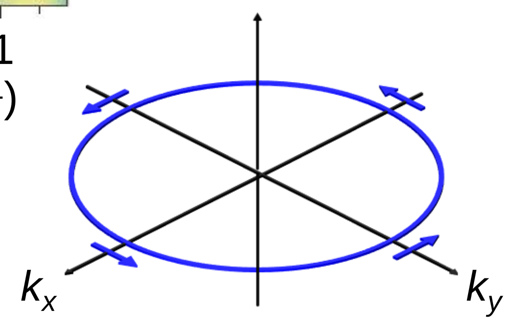

Edelstein (EE) and Inverse Edelstein Effect (IEE)

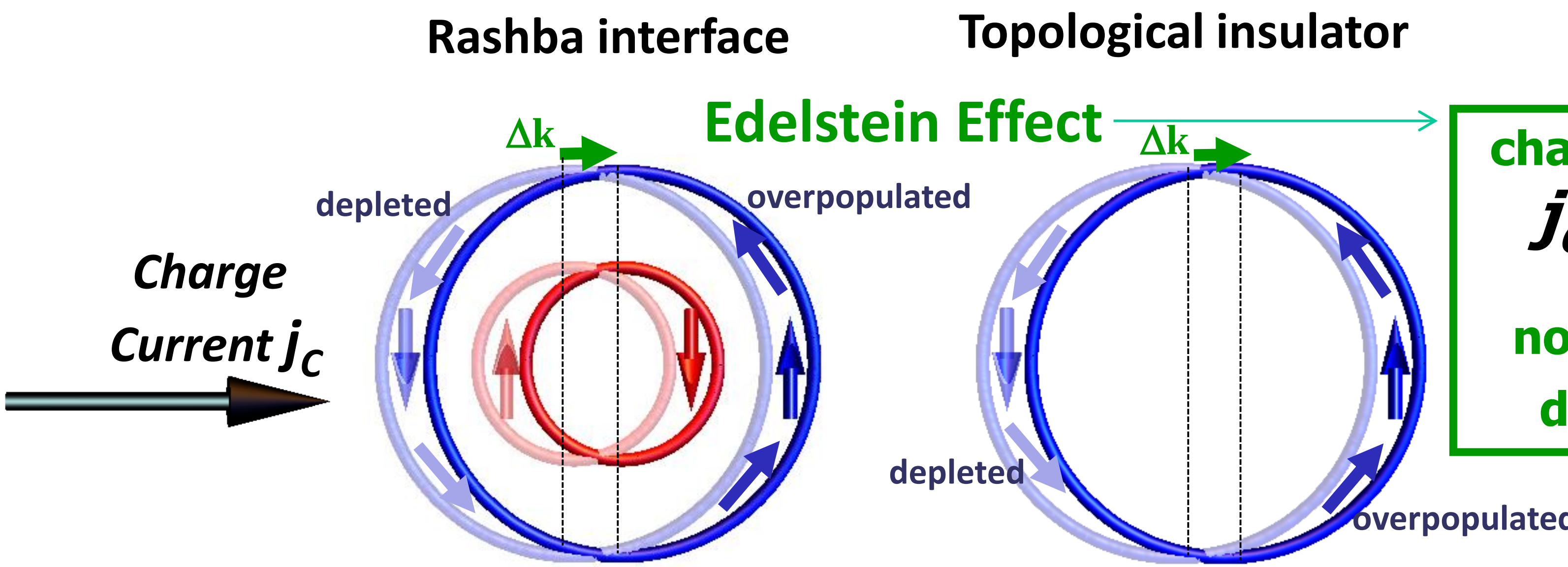

charge current j_C in 2DEG induces nonzero spin density σ_y

Edelstein (EE) and Inverse Edelstein Effect (IEE)

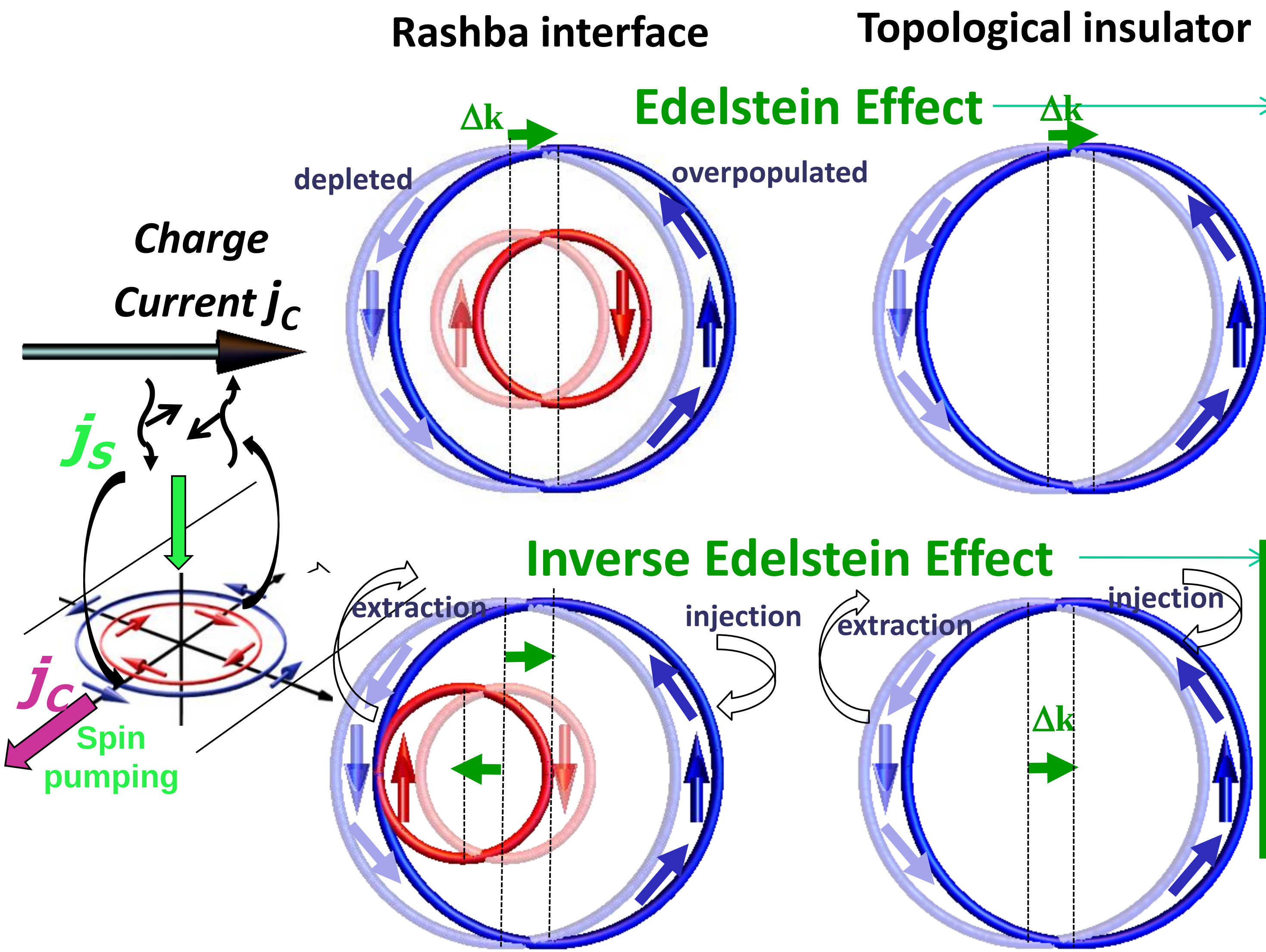

charge current j_c in 2DEG induces nonzero spin density σ_y

Injection of spin current j_s induces charge current j_c

Edelstein (EE) and Inverse Edelstein Effect (IEE)

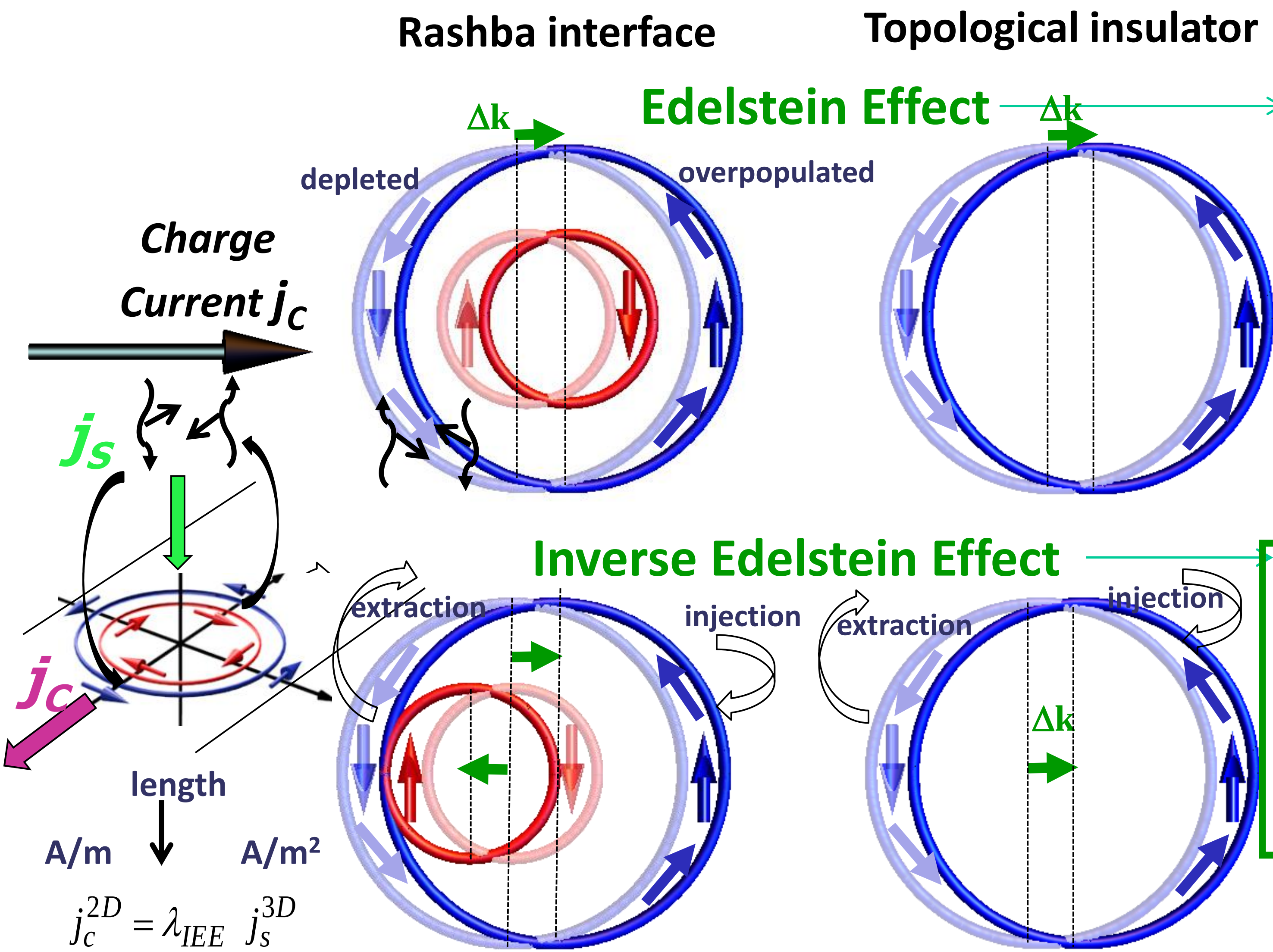

$$j_c^{2D} = \lambda_{IEE}\ j_s^{3D}$$

$$\text{with}\ \ \lambda_{IEE} = \frac{\alpha_R\, \tau}{\hbar}$$

charge current j_c in 2DEG induces nonzero spin density σ_y

Injection of spin current j_s induces charge current j_c

Rojas-Sanchez, AF et al, Nat.Com. 013, Shen et al, PRL014

Edelstein (EE) and Inverse Edelstein Effect (IEE)

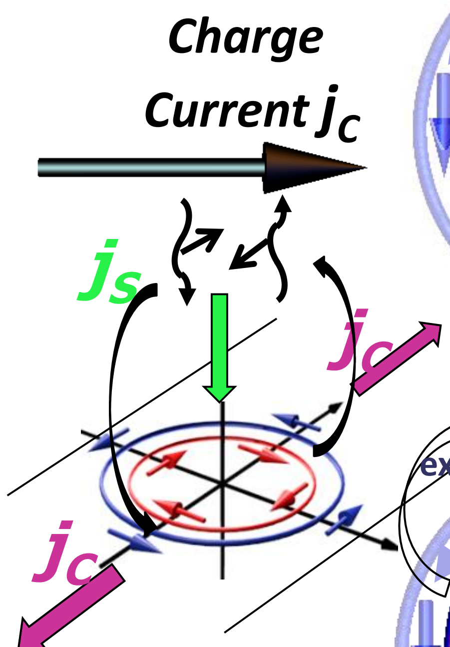

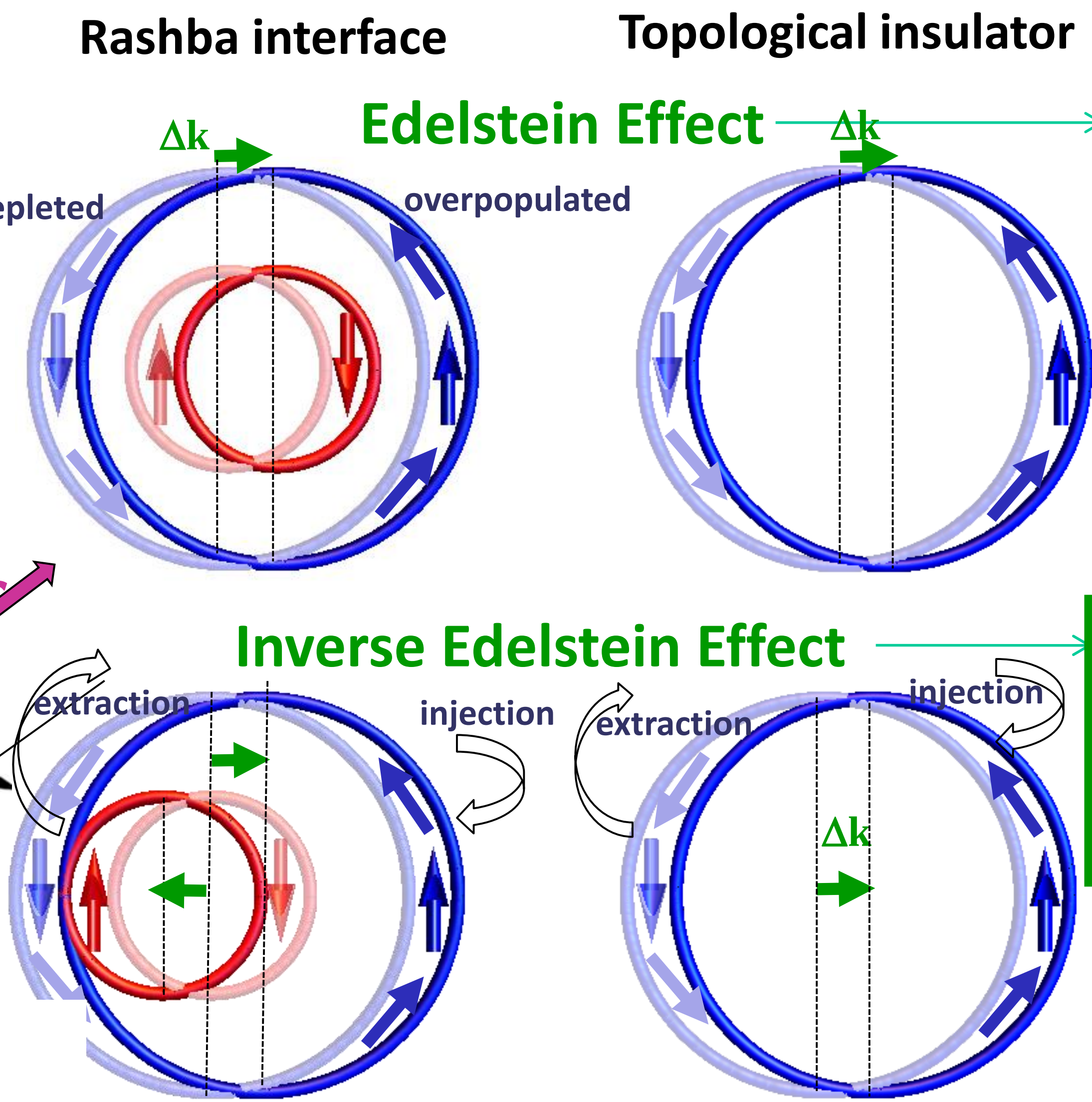

charge current j_c in 2DEG induces nonzero spin density σ_y

Injection of spin current j_s induces charge current j_c

Rashba interface:

length

A/m A/m²

$$j_c^{2D} = \lambda_{IEE} \; j_s^{3D}$$

$$\text{with } \lambda_{IEE} = \frac{\alpha_R \tau}{\hbar}$$

Topological insulator:

length

A/m A/m²

$$j_c^{2D} = \lambda_{IEE} \; j_s^{3D}$$

$$\text{with } \lambda_{IEE} = v_F \tau$$

Rojas-Sanchez et al, PRL 116, 096602 (2016), Culcer, Physica012

Edelstein (EE) and Inverse Edelstein Effect (IEE)

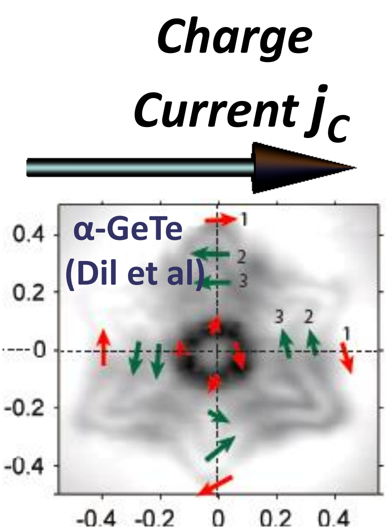

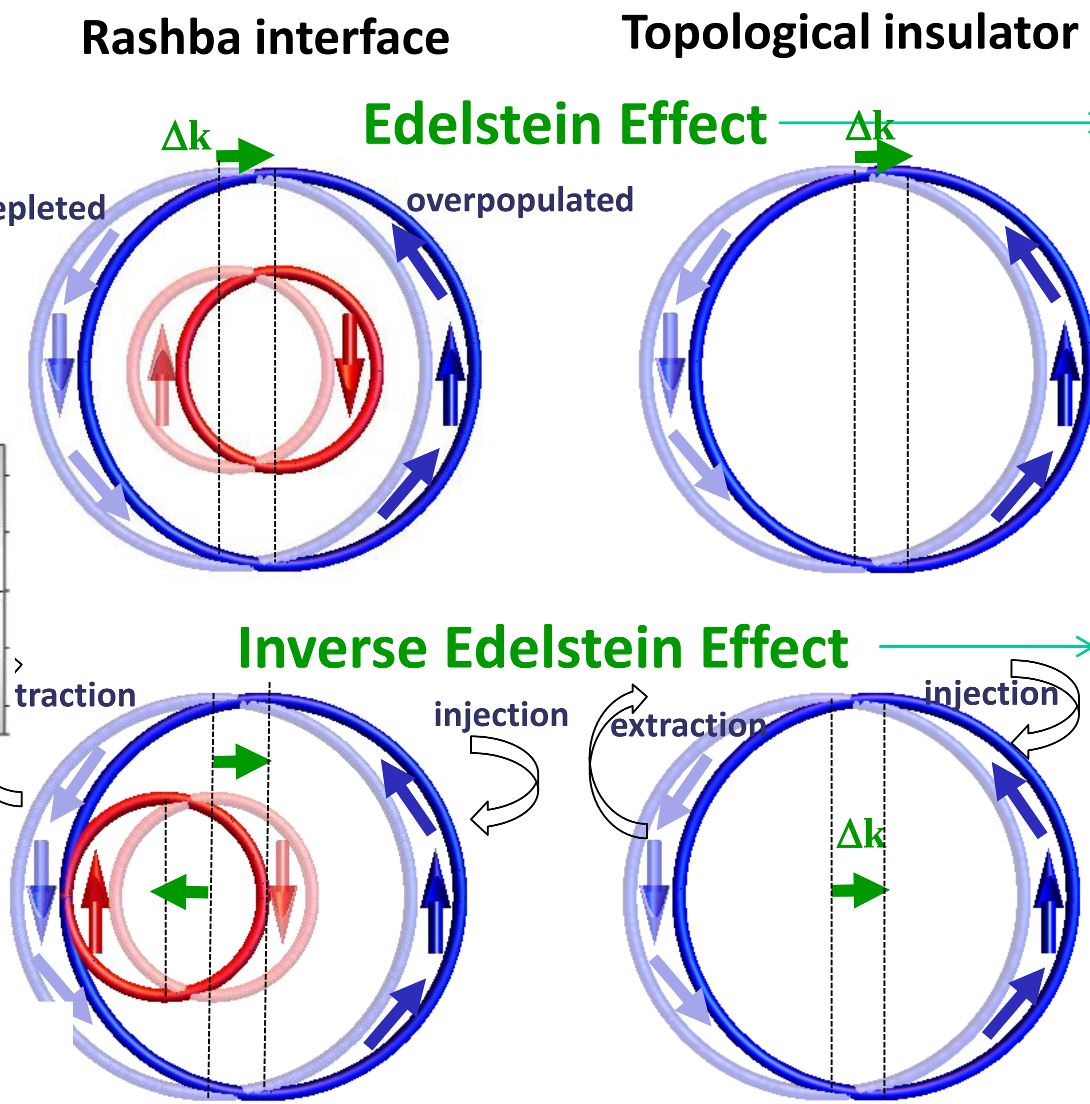

charge current j_c in 2DEG induces nonzero spin density σ_y

Injection of spin current j_s induces charge current j_c

Rashba interface:

length

A/m ↓ A/m²

$$j_c^{2D} = \lambda_{IEE} \; j_s^{3D}$$

$$\text{with } \lambda_{IEE} = \frac{\alpha_R \tau}{\hbar}$$

Topological insulator:

length

A/m ↓ A/m²

$$j_c^{2D} = \lambda_{IEE} \; j_s^{3D}$$

$$\text{with } \lambda_{IEE} = v_F \tau$$

Rojas-Sanchez et al, PRL 116, 096602 (2016), Culcer, Physica012

Inverse Edelstein effect (IEE) in spin pumping experiments

- Bi/Ag interface* (**J-C. Rojas-Sanchez, AF et al, Nature Communications, 4, 2944, 2013)**
- **Other examples presented today:**
- topological 2DEG: α-Sn and LAO/STO interface

* Before Bi/Ag, first observed in n-GaAs-AlGaAs QW, Ganichev et al, Nature 417, 153, 2002

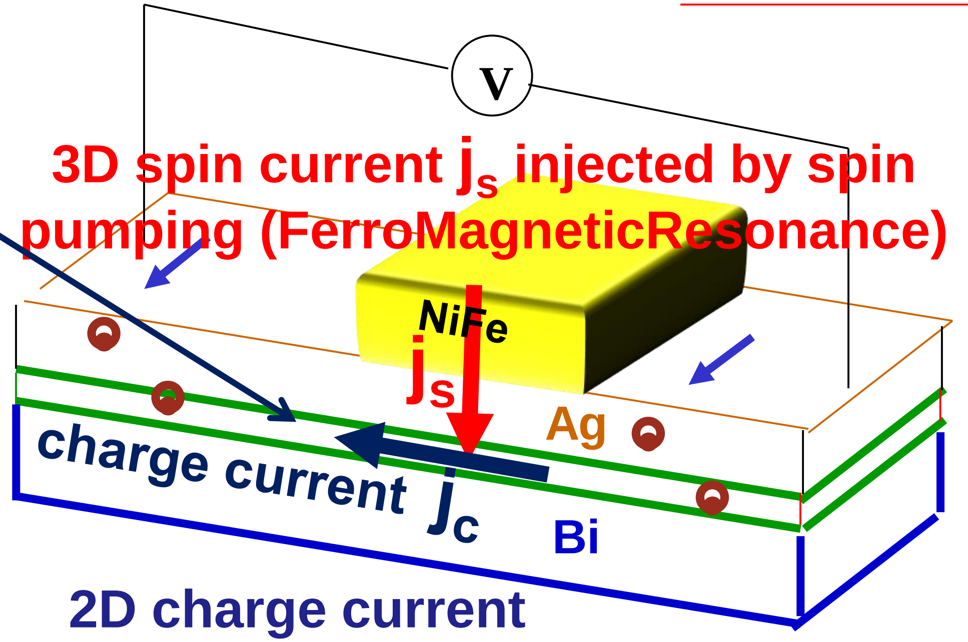

2D charge current derived from V

Spin to charge conversion by Bi/Ag Rashba interfaces

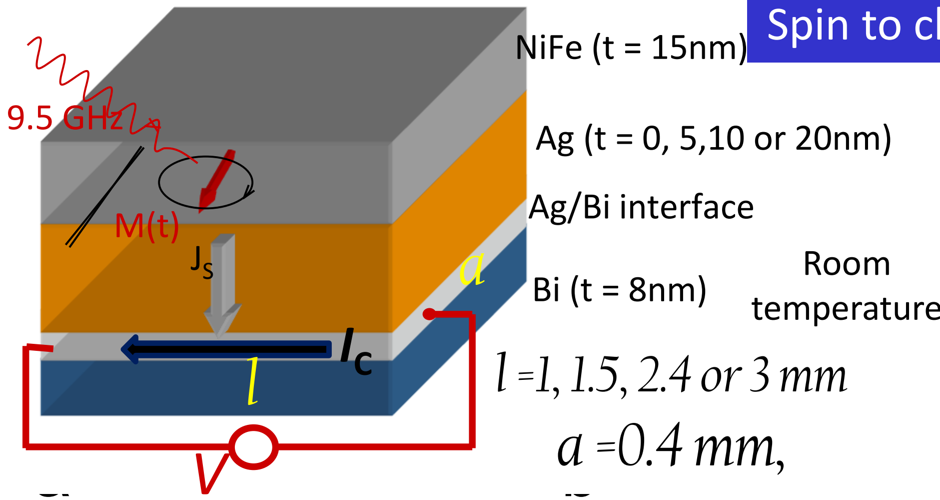

$I_C = \frac{V}{R_\square l}$ *is* large *only when there is a Bi / Ag* interface

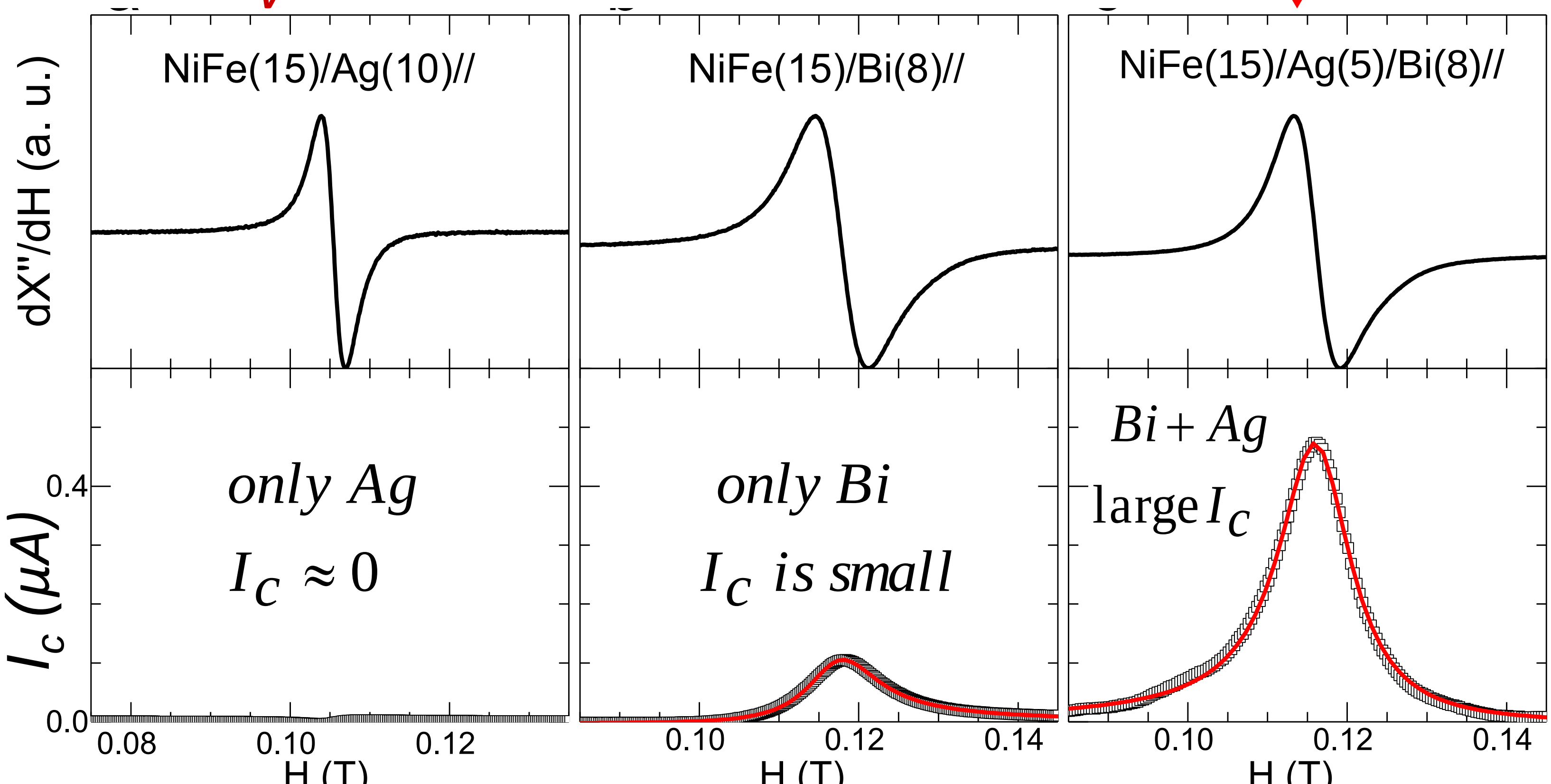

J-C. Rojas-Sanchez, AF et al, Nature Communications, 4, 2944, 2013

Spin to charge conversion by Bi/Ag Rashba interfaces

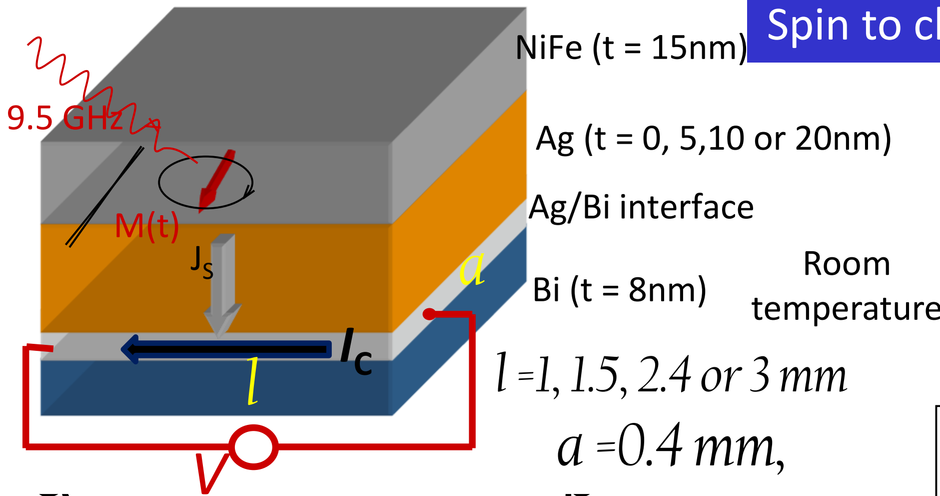

$$I_C = \frac{V}{R_{\square} l} \text{ is large}$$

only when there is a Bi / Ag interface

S. Sangiao et al. APL 106, 172403 (2015)
as expected by Rashba symmetry,
I_c has opposite signs for, respectively,
Ag above Bi and Ag under Bi

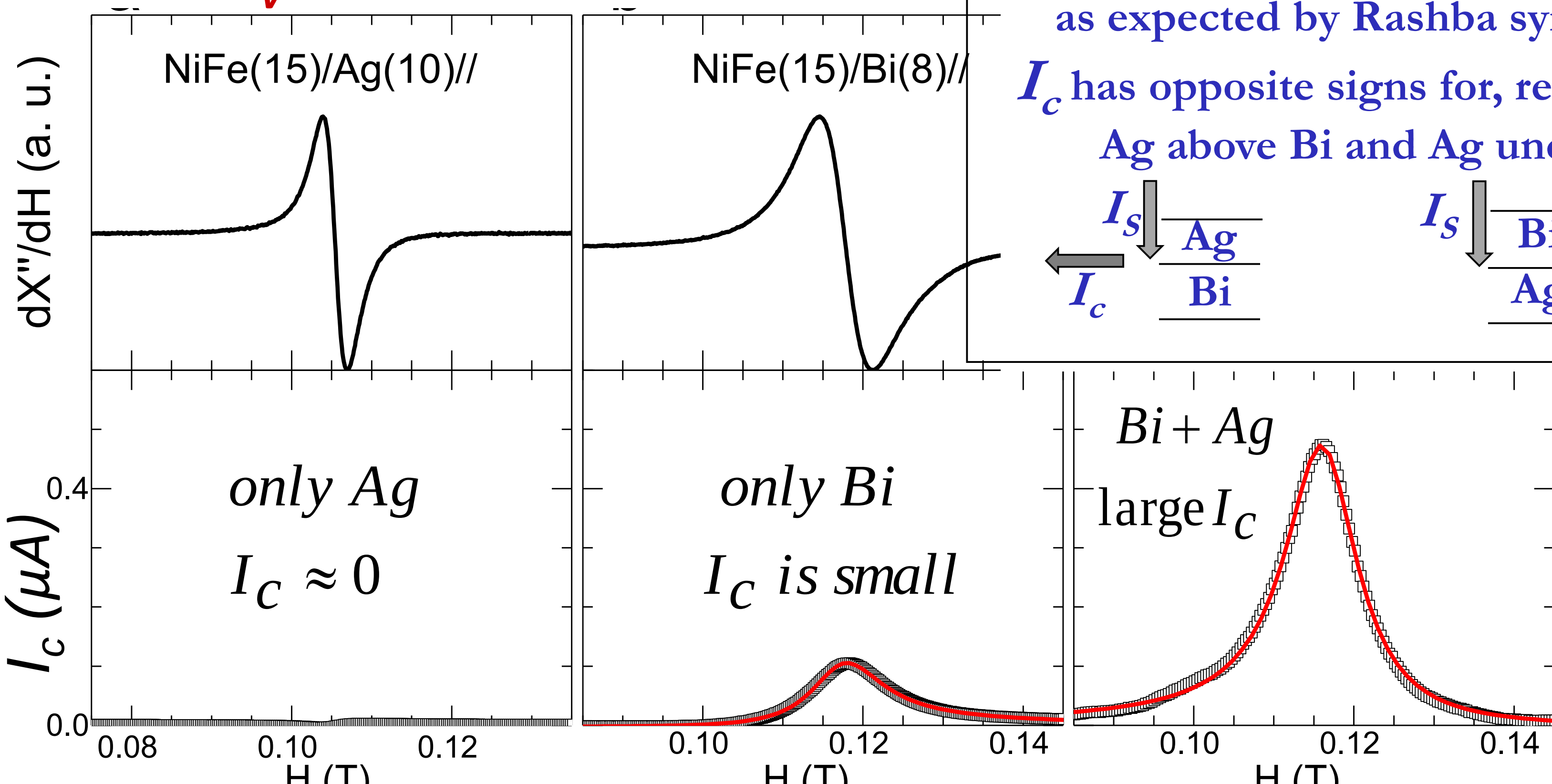

J-C. Rojas-Sanchez, AF et al, Nature Communications, 4, 2944, 2013

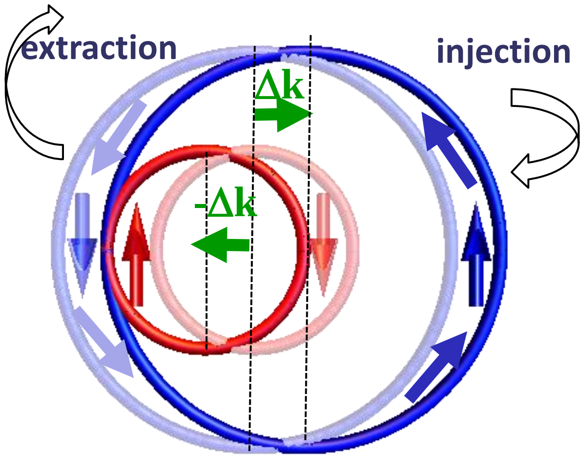

$$\underset{(A/m^2)}{\overset{(A/m)}{\frac{j_c}{j_s}}} = \lambda_{IEE}^{Bi/Ag} = \frac{\alpha_R \tau}{\hbar}$$

J-C. Rojas-Sánchez et al. Nature Comm. 2013

(Similar results by K. Shen, R. Raimondi et al, PRL. 2014)

Other results on Bi/Ag: Nomura et al, APL 2015

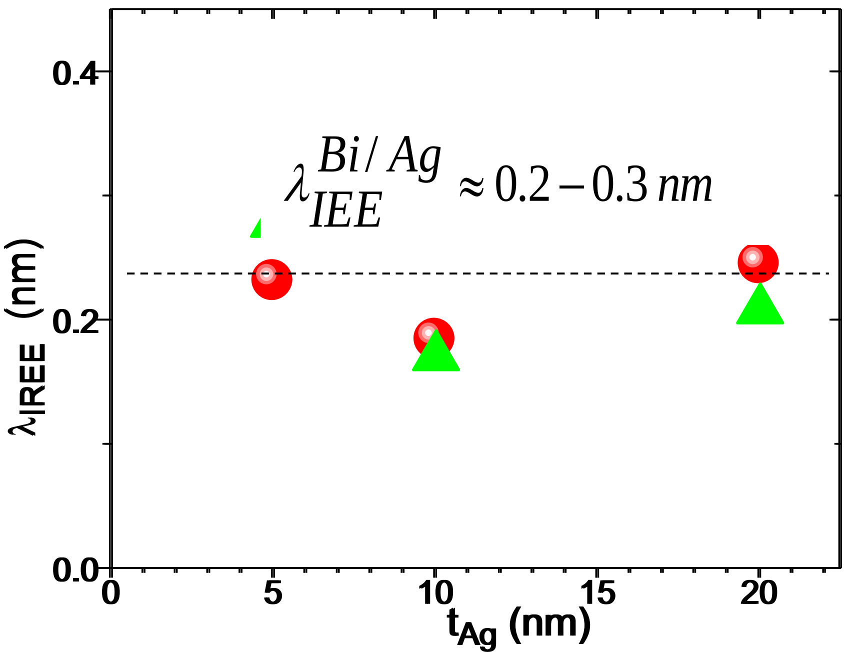

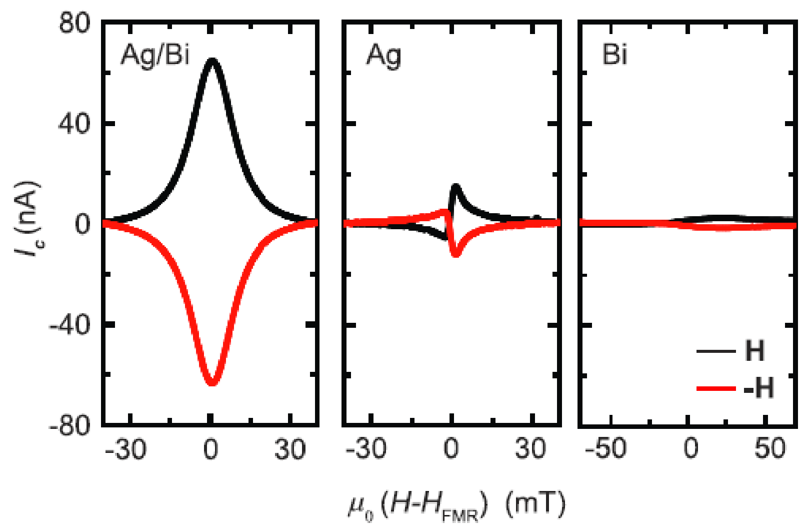

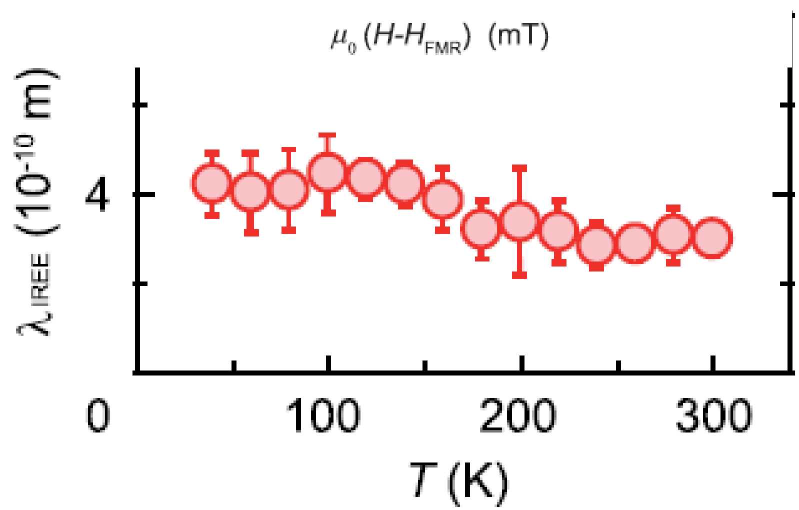

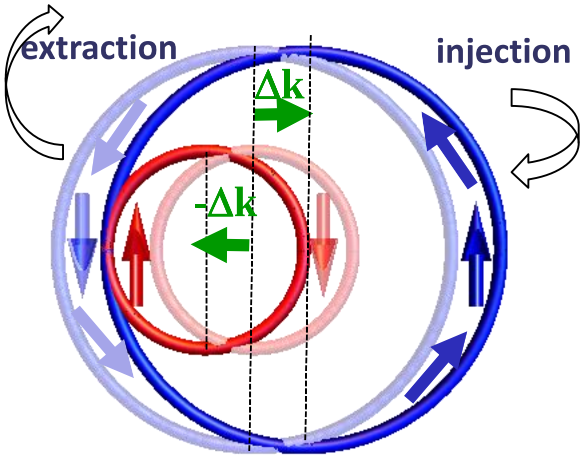

$$\underset{(A/m^2)}{\overset{(A/m)}{\frac{j_c^{2D}}{j_s^{3D}}}} = \lambda_{IEE}^{Bi/Ag} = \frac{\alpha_R \tau}{\hbar}$$

J-C. Rojas-Sánchez et al. Nature Comm. 2013

(Similar results by K. Shen, R. Raimondi et al, PRL. 2014)

More recent results on Bi/Ag, Sb/Ag..

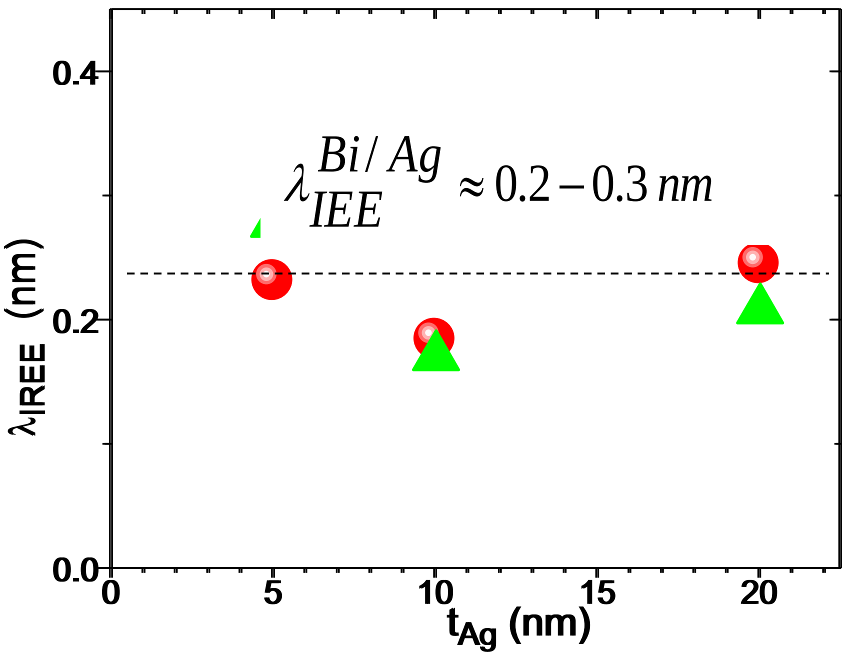

W. Zhang et al. JAP 117, 17C727 (2015)

λ_{IEE}(Ag/Bi) ~ 0.1nm >$_{I}\lambda_{IEE}$(Ag/Sb) ~0.03 nm 0.1nm

Sisasa et al, 2015, λ_{IEE}(Cu/Bi) derived from LSV is small and its sign changes with T

Spin to charge current conversion at Ag/IrO_2 (Fujiwara, Otani et al, Nat Comm. 2013,DOI: 10.1038/ncomms3893)and Cu/Bi_2O_3 interfaces (Karube, Otani et al, App.Phys. Expr. 9,033001)

Zhang et al (PRL 2015), Jungfleisch et al (ArXiv 1500.0141): measurement of charge to spin conversion (direct EE) at Bi/Ag interface

Spin to charge conversion by Dirac cone states with helical spin polarization of α-Sn

PRL 111, 136804 (2013)

Large-Gap Quantum Spin Hall Insulators in Tin Films

Yong Xu,[1,2] Binghai Yan,[3] Hai-Jun Zhang,[1] Jing Wang,[1] Gang Xu,[1] Peizhe Tang
Wenhui Duan,[2] and Shou-Cheng Zhang[1,2,*]

PHYSICAL REVIEW B 90, 125312 (2014)

DFT
44ML

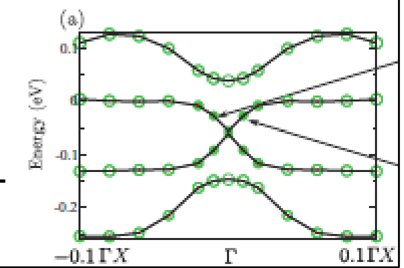

Elemental Topological Insulator with Tunable Fermi Level: Strained α-Sn on InSb(001)

A. Barfuss,[1] L. Dudy,[1] M. R. Scholz,[1] H. Roth,[1] P. Höpfner,[1] C. Blumenstein,[1] G. Landolt,[2,3] J. H. Dil,[2,3]
N. C. Plumb,[2] M. Radovic,[2] A. Bostwick,[4] E. Rotenberg,[4] A. Fleszar,[5] G. Bihlmayer,[6] D. Wortmann,[6]
G. Li,[5] W. Hanke,[5] R. Claessen,[1] and J. Schäfer[1,*]

PRL 111, 157205 (2013)

PRL 111, 216401 (2013)

Dirac Cone with Helical Spin Polarization in Ultrathin α-Sn(001) Films

Yoshiyuki Ohtsubo,[1,*] Patrick Le Fèvre,[1] François Bertran,[1] and Amina Taleb-Ibrahimi[1,2,†]

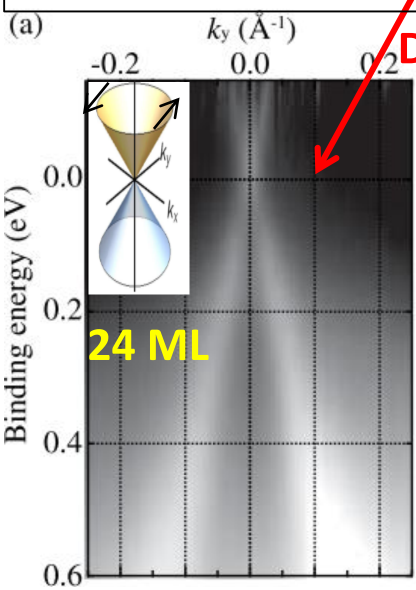

Dirac-cone with helical spin polarization

ARPES: Y. Ohtsubo et al. PRL 11, 216401 (2013)

InSb//α-Sn(24-30ML)

υ_F = 7.3 10^5 m/s (4.8 evÅ)

Casiopee beam line at SOLEIL, Room temperature

Our α-Sn/Fe and α-Sn/Ag/Fe samples (α-Sn:30ML) have been grown in the same conditions in situ on the same beam line to check by ARPES if the topological states are or are not kept after depositing Fe or Ag for our spin pumping experiments

First stage : ARPES in α-Sn(30ML) + Fe or αSn(30ML)+Ag

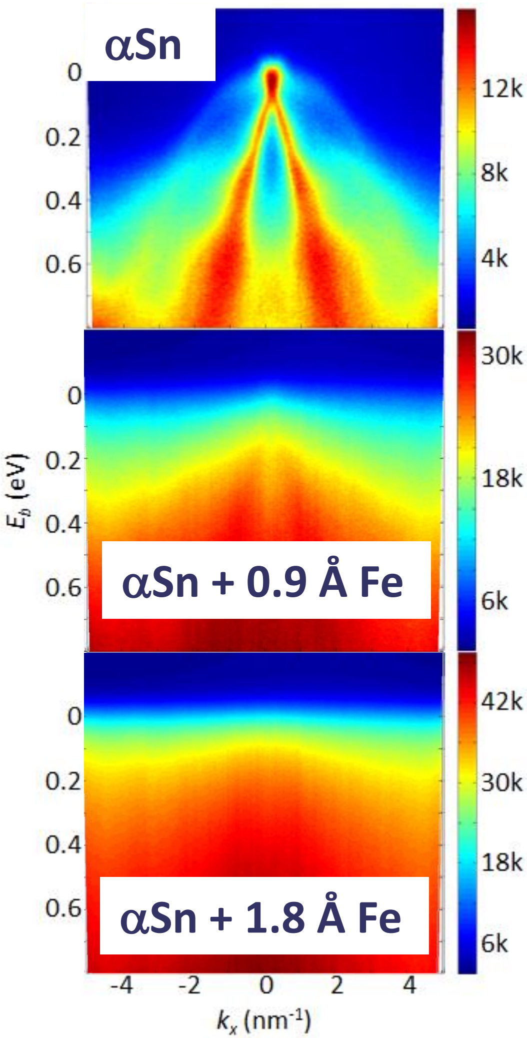

Room temperature

Rojas-Sanchez et al, PRL 116, 096602 (2016)

First stage : ARPES in α-Sn(30ML) + Fe or αSn(30ML)+Ag

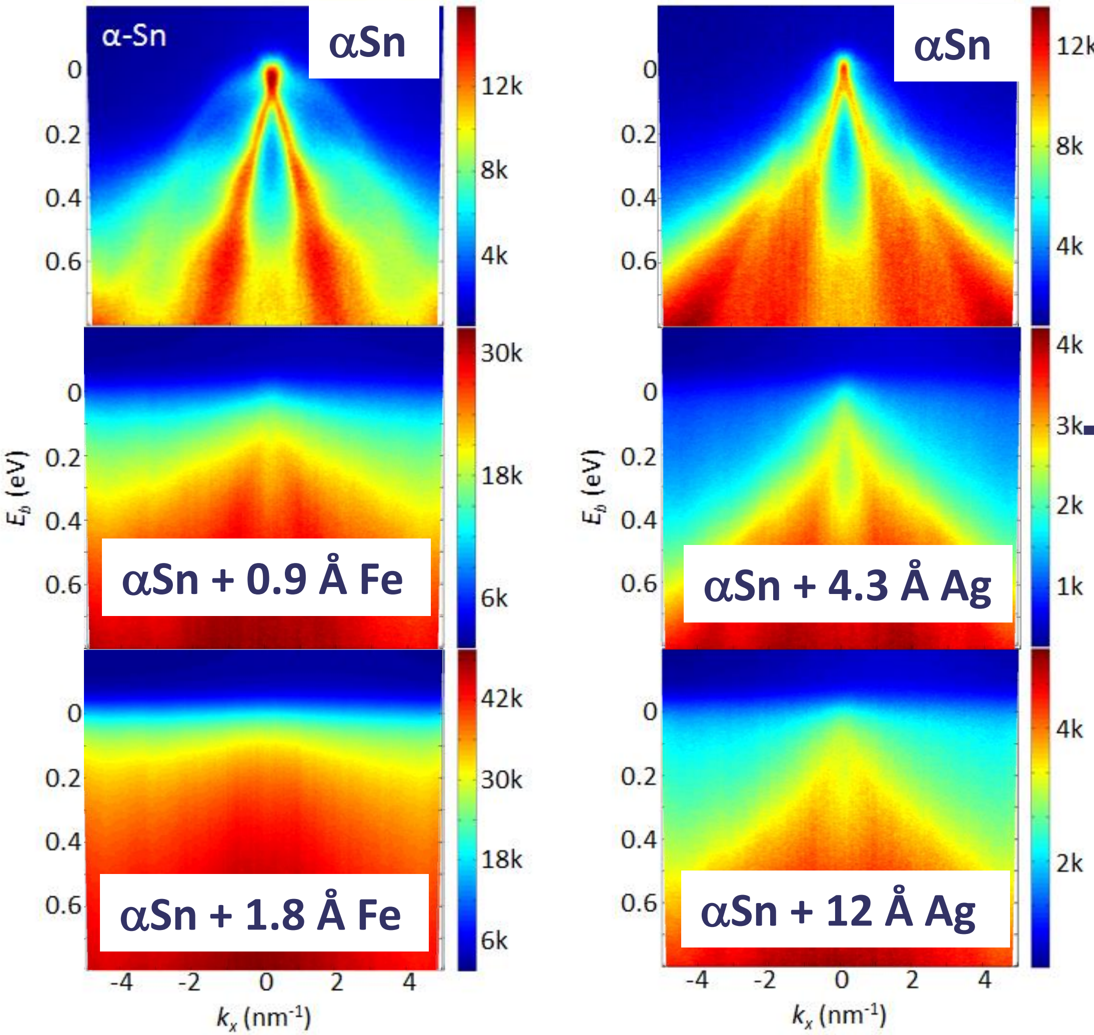

→ The Dirac cone remains when adding Ag on Sn

↓

IEE expected in spin pumping from Fe into Ag/Sn bilayers

Room temperature

Rojas-Sanchez et al, PRL 116, 096602 (2016)

Spin pumping on α-Sn/Fe and α-Sn/Ag(2nm)/Fe

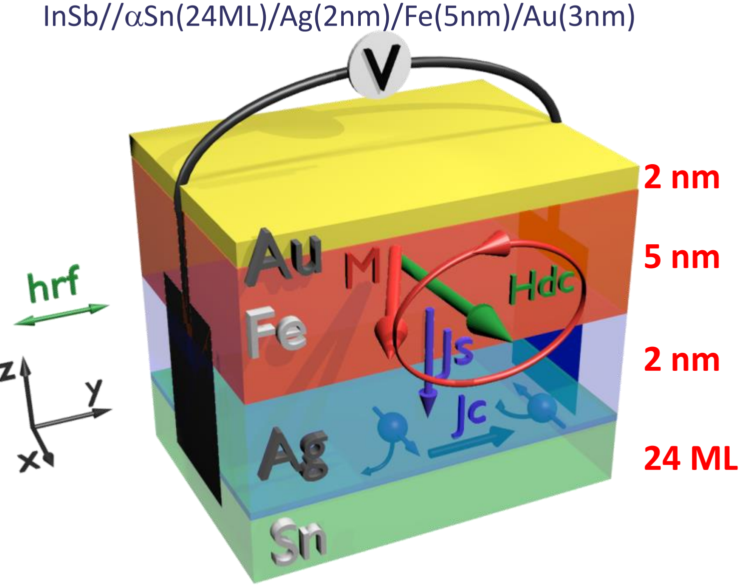

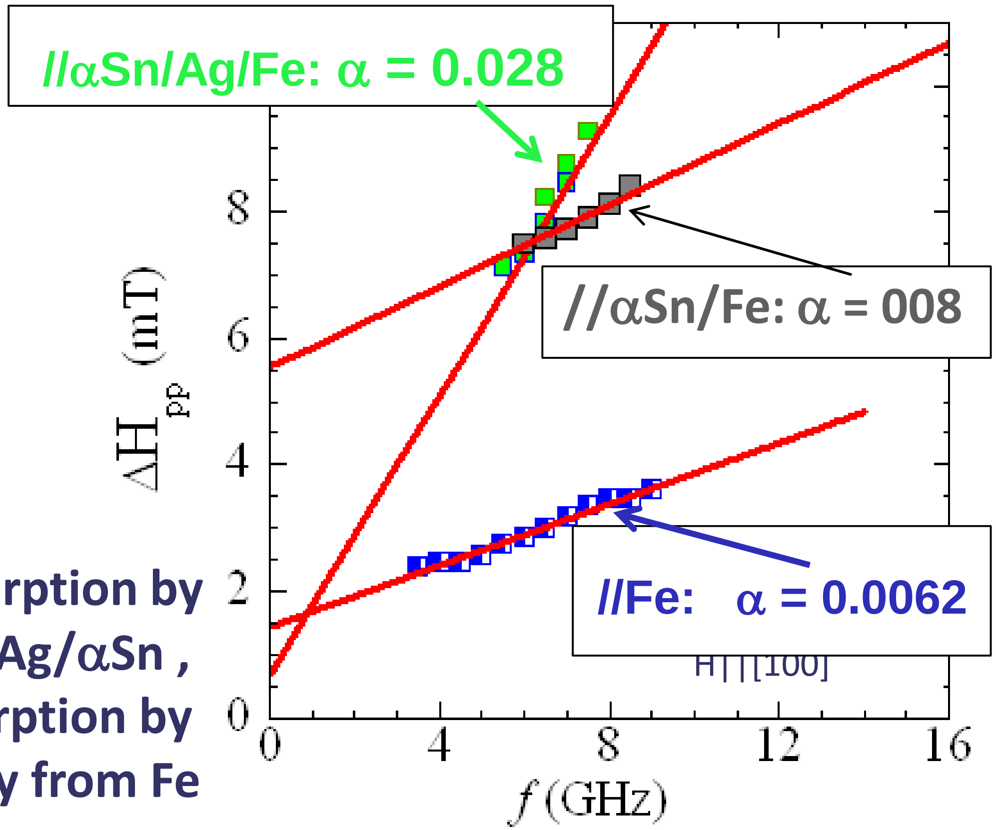

strong spin absorption by pumping Fe on Ag/αSn , weak spin absorption by pumping directly from Fe an αSn

Rojas-Sanchez et al, PRL 116, 096602 (2016)

Spin pumping on α-Sn/Fe and α-Sn/Ag(2nm)/Fe

InSb//αSn(24ML)/Ag(2nm)/Fe(5nm)/Au(3nm)

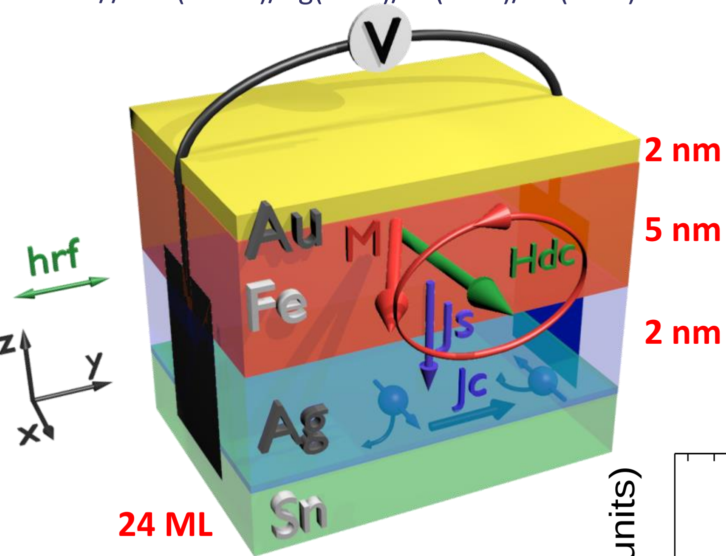

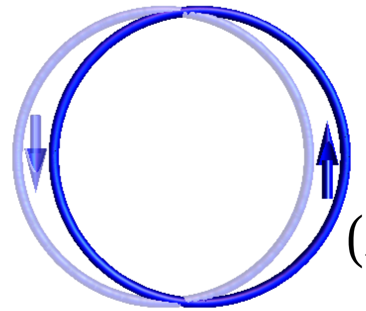

$$\frac{j_c\ (A/m)}{j_s\ (A/m^2)} = \lambda_{IEE}^{TI} = v_F \tau$$

$$\lambda_{IEE}^{\alpha-Sn} \cong 2.1\,nm$$

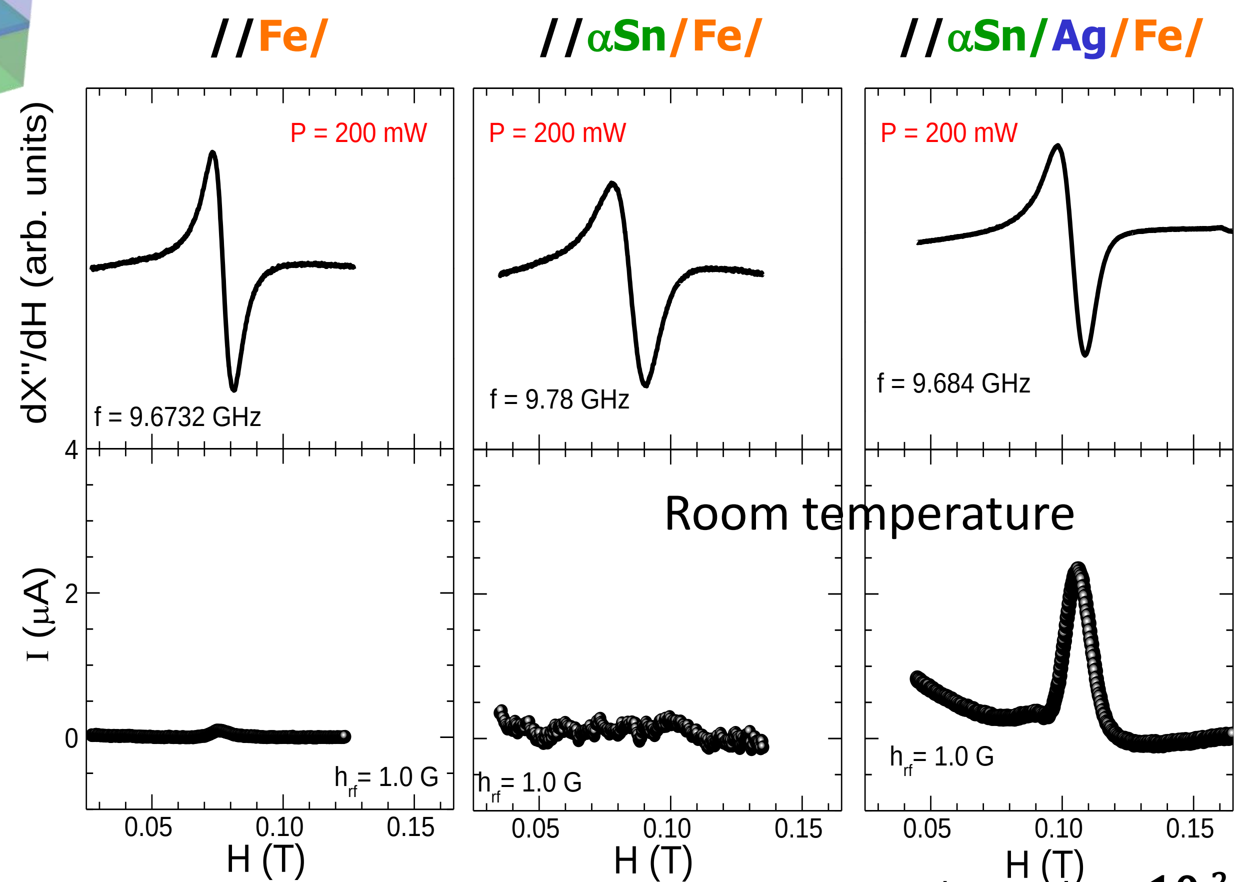

Rojas-Sanchez et al,
PRL 116, 096602 (2016)

Precession angle ≃ 10^{-2}

Spin pumping on α-Sn/Fe and α-Sn/Ag(2nm)/Fe

InSb//αSn(24ML)/Ag(2nm)/Fe(5nm)/Au(3nm)

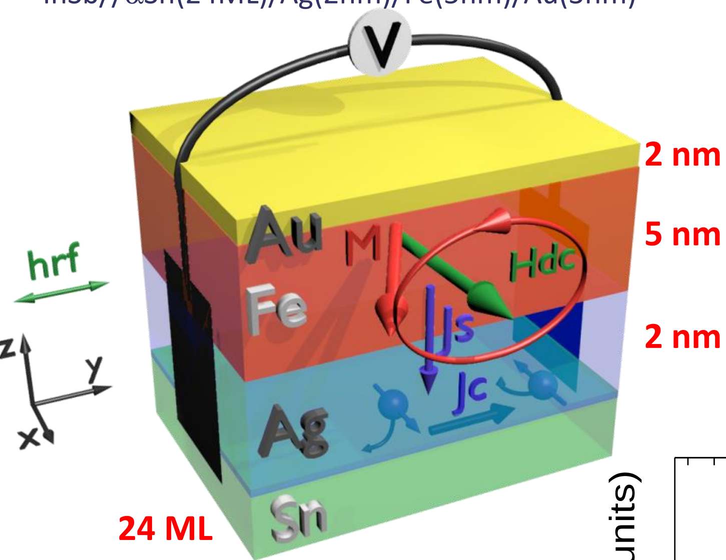

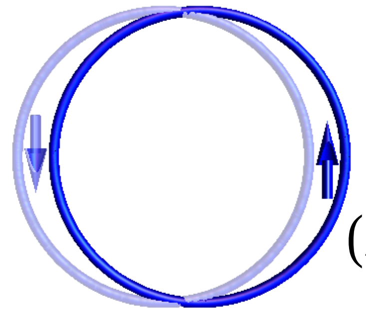

$$\frac{j_c}{j_s} = \lambda_{IEE}^{TI} = v_F \tau$$

j_c: (A/m); j_s: (A/m^2)

$$\lambda_{IEE}^{\alpha-Sn} \cong 2.1\, nm$$

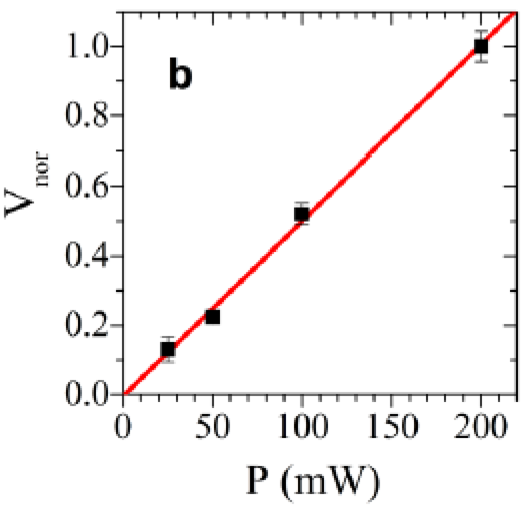

Rojas-Sanchez et al,
PRL 116, 096602 (2016)

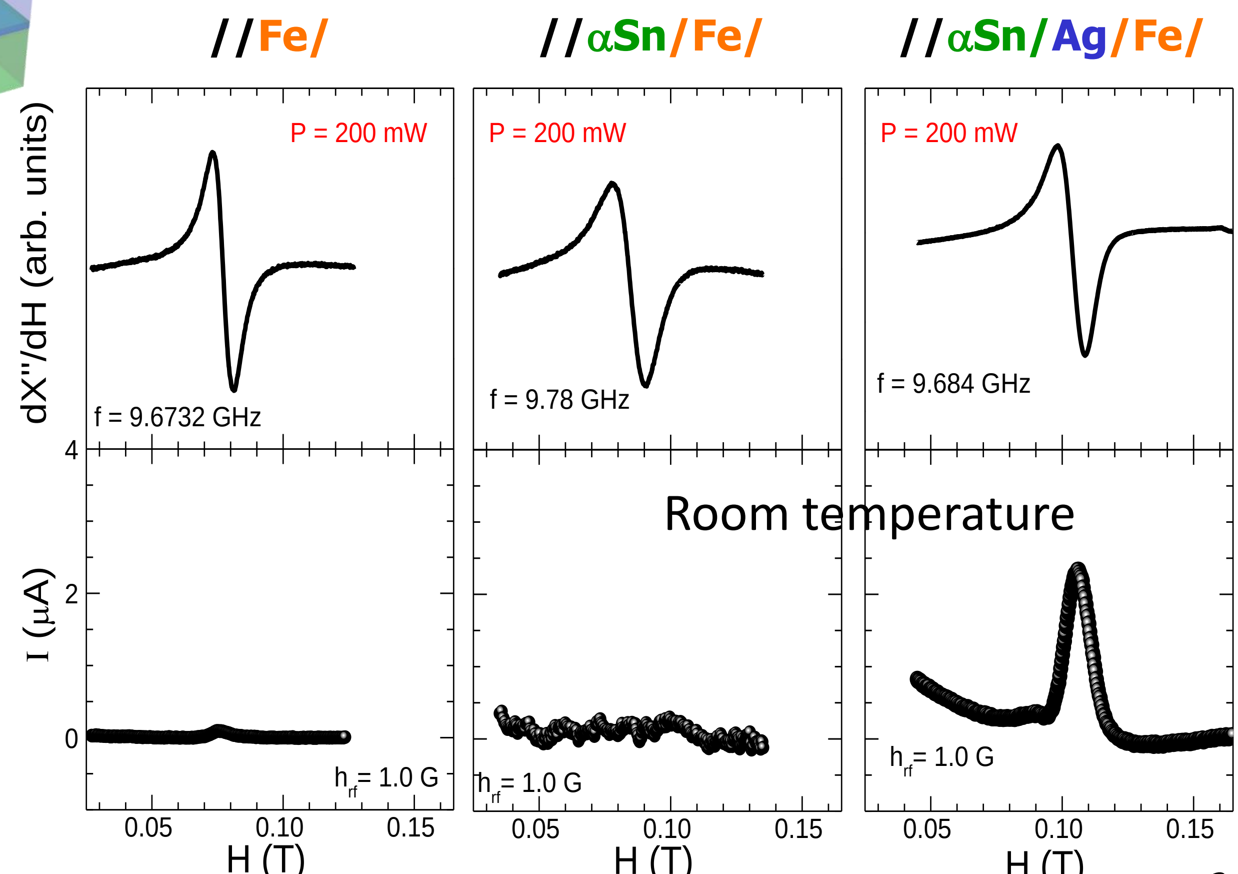

Precession angle ≃ 10^{-2}

Spin pumping on α-Sn/Fe and α-Sn/Ag(2nm)/Fe

InSb//αSn(24ML)/Ag(2nm)/Fe(5nm)/Au(3nm)

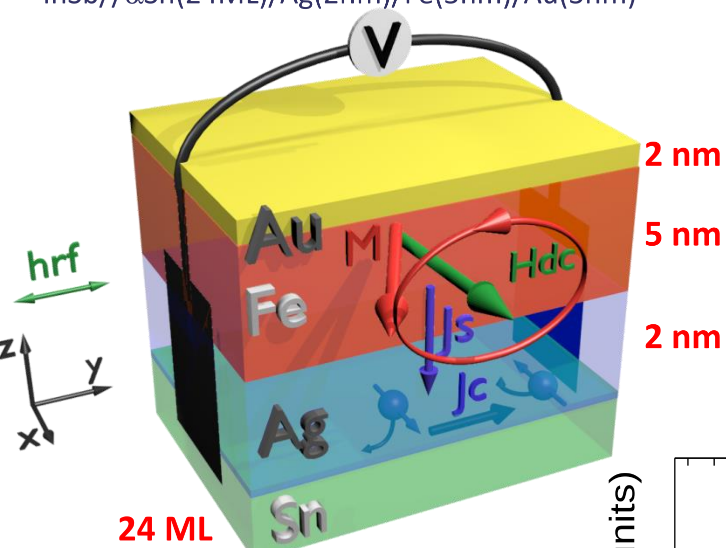

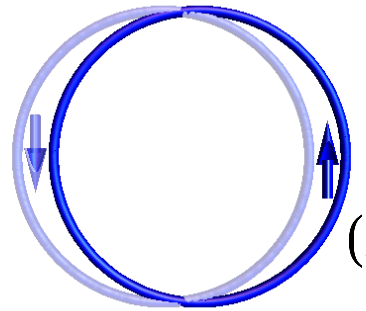

$$\frac{j_c \;(A/m)}{j_s \;(A/m^2)} = \lambda_{IEE}^{TI} = v_F \tau$$

$$\lambda_{IEE}^{\alpha-Sn} \cong 2.1\, nm$$

λ_{IEE} >0 in agreement with CCW chirality in upper cone (from spin-resolved ARPES)

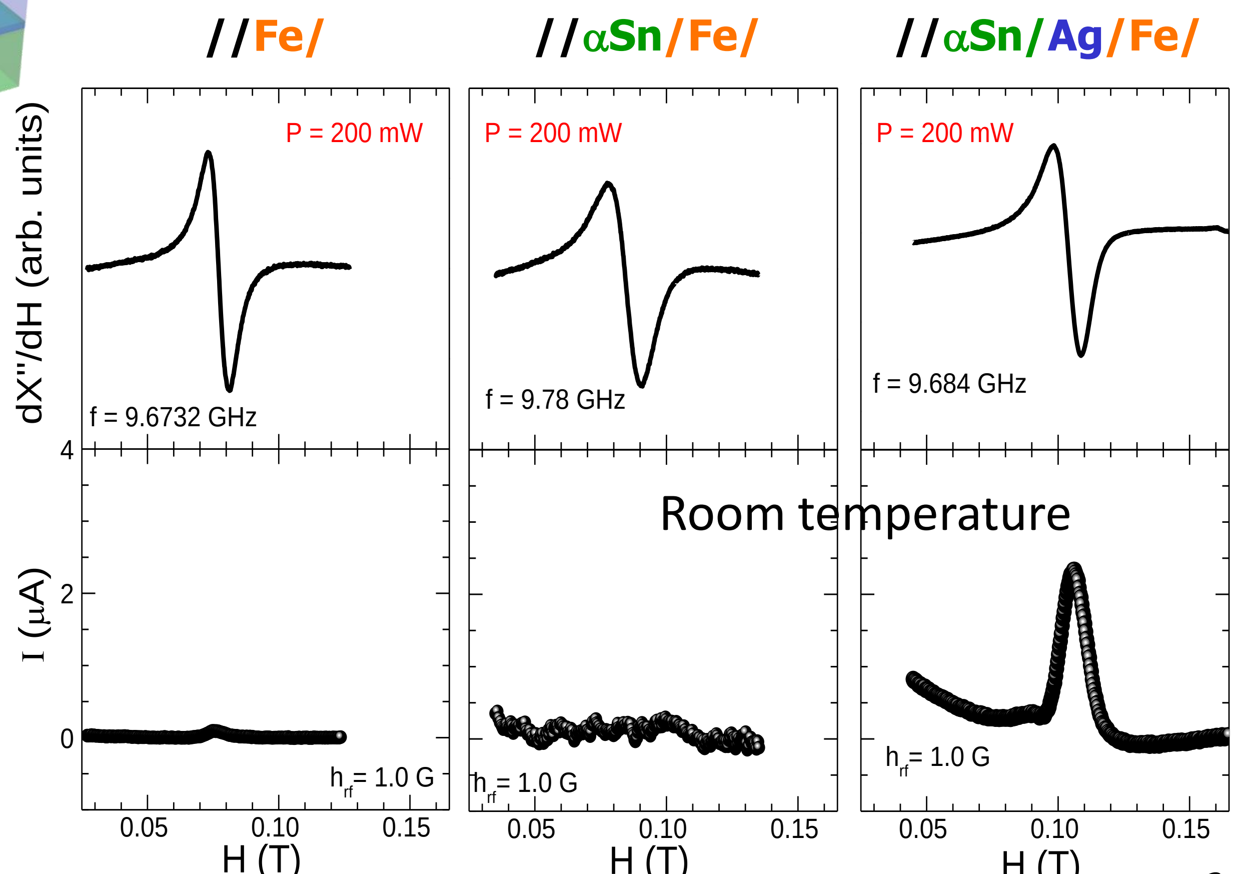

Precession angle ≃ 10^{-2}

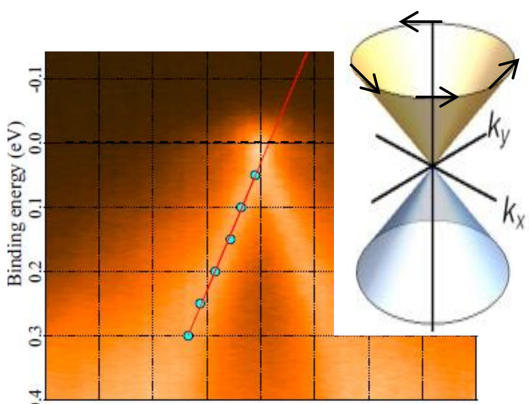

Rojas-Sanchez et al, PRL 116, 096602 (2016)

Spin pumping on α-Sn/Fe and α-Sn/Ag(2nm)/Fe

InSb//αSn(24ML)/Ag(2nm)/Fe(5nm)/Au(3nm)

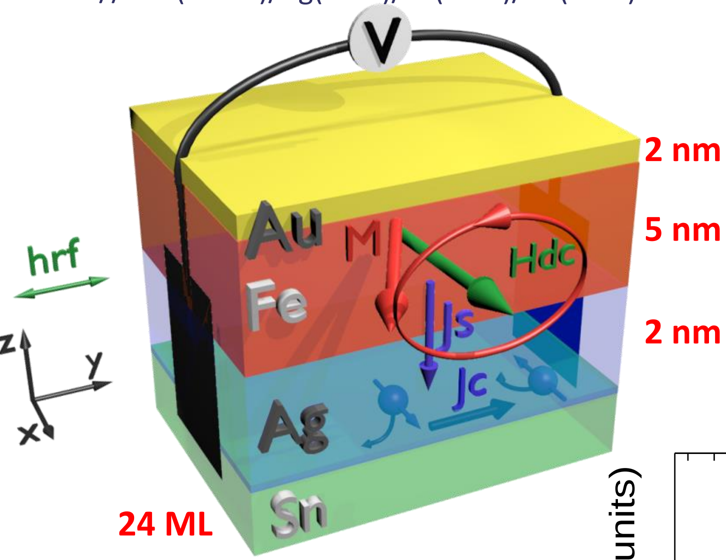

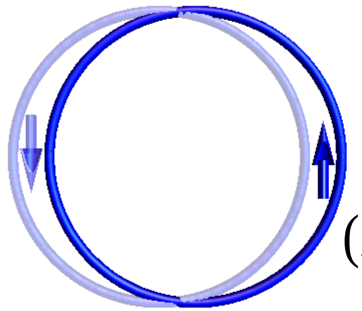

$$\frac{j_c \;(A/m)}{j_s \;(A/m^2)} = \lambda_{IEE}^{TI} = v_F \tau$$

$$\lambda_{IEE}^{\alpha-Sn} \cong 2.1\, nm$$

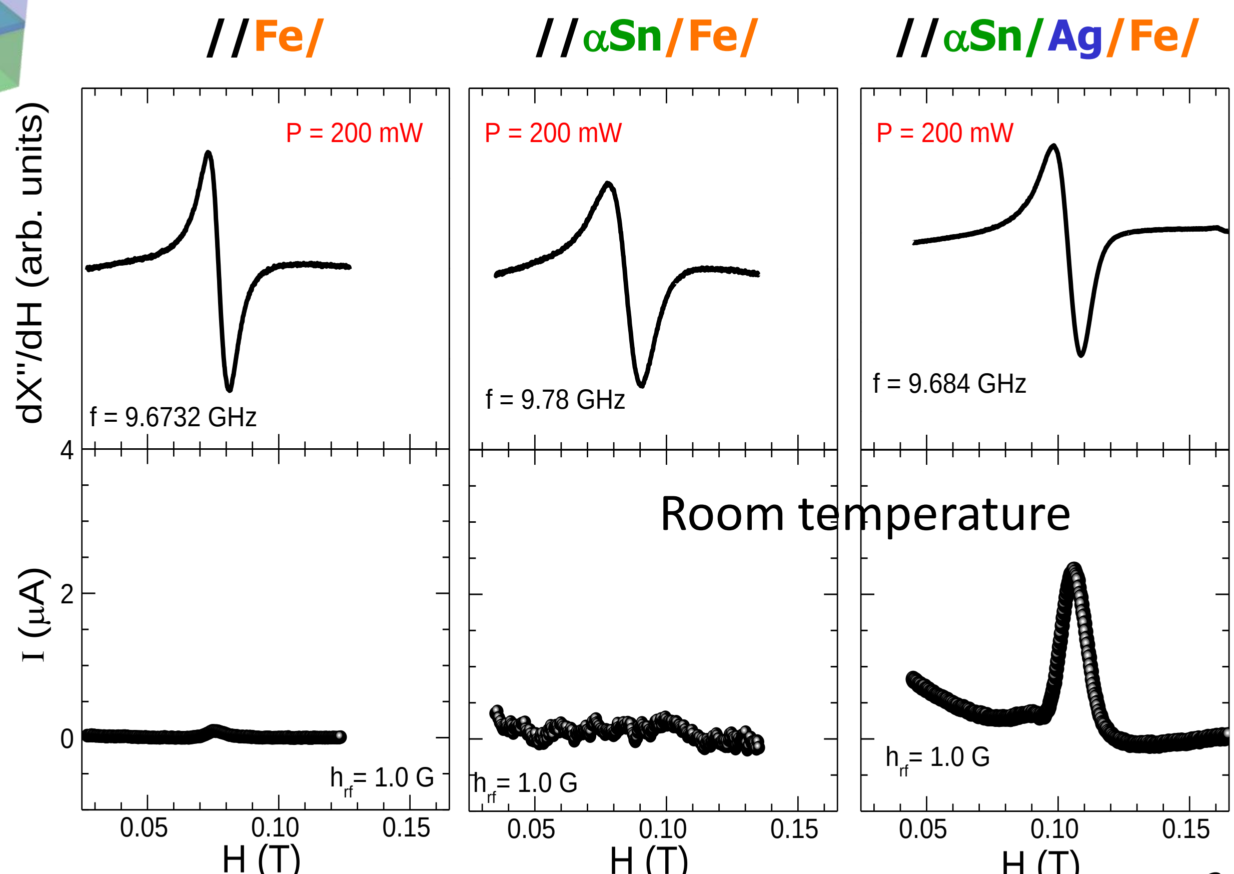

Room temperature

Precession angle ≃ 10^{-2}

In progress, dependence on T, **α**-Sn thickness, gate voltage, applied field + inverse conversion

Other spin/charge conversions with TI,
e.g **Shiomi et al, PRL014,**
Jamali et al NanoLetters 015
(spin pumping),
Tang et al, Nano Letters 014,
(electrical spin inject.)

Relaxation time τ of out-of-equilibrium distribution in topological states

For circular contours

$$\lambda_{IEE} = v_F \, \tau = 2.1nm, \qquad v_F \cong 0.56 \times 10^6 m/s$$

$$\rightarrow \quad \tau \cong 3.7 fs \quad (Bi/Ag : \tau \cong 5 fs)$$

$v_F \cong 0.56 \times 10^6 m/s$

$for\ cone\ at\ Ag/Sn\ with\ Ag = 0.23nm$

$(0.6 \times 10^6 m/s\ \ for\ \ free\ Sn)$

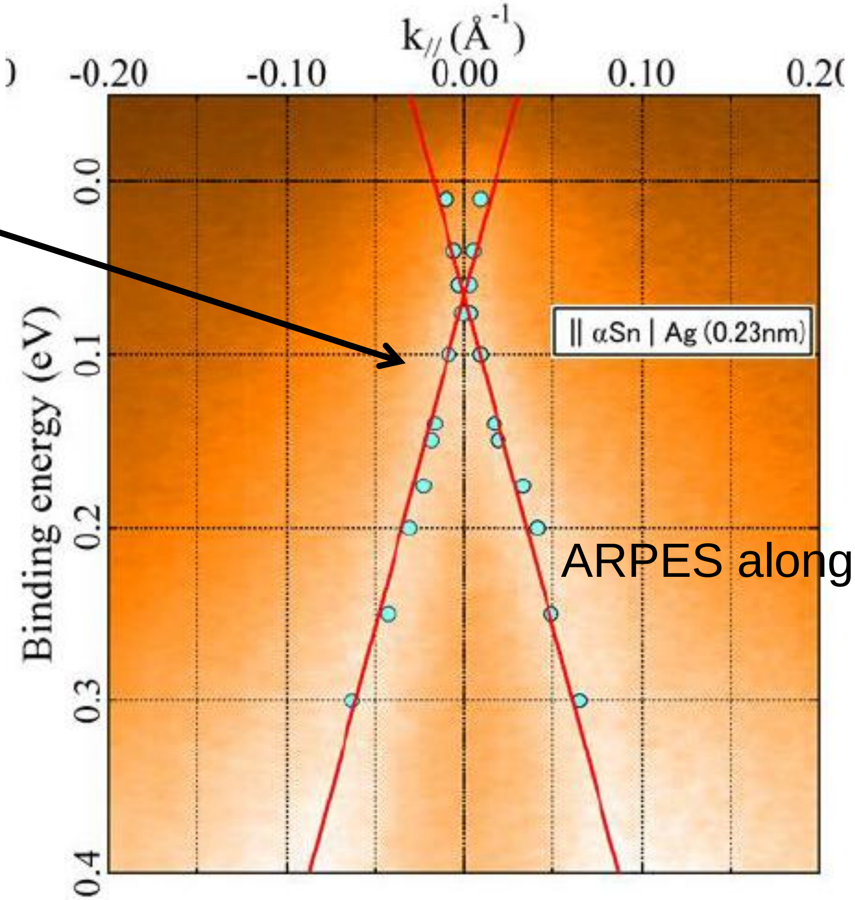

ARPES along 110

Dots correspond to maximum intensity in E=cst scans

Rojas-Sanchez et al,
PRL 116, 096602 (2016)

Relaxation time τ of out-of-equilibrium distribution in topological states

For circular contours

$$\lambda_{IEE} = v_F \tau = 2.1 nm, \quad v_F \cong 0.56 \times 10^6 m/s$$

$$\rightarrow \quad \tau \cong 3.7 fs \quad (Bi/Ag : \tau \cong 5 fs)$$

ARPES intensity mapping in (k_x, k_y) plane (low resolution)

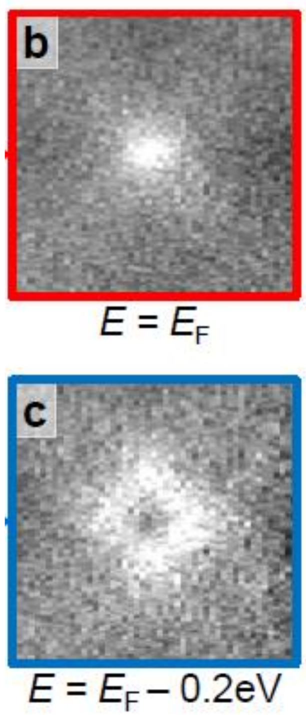

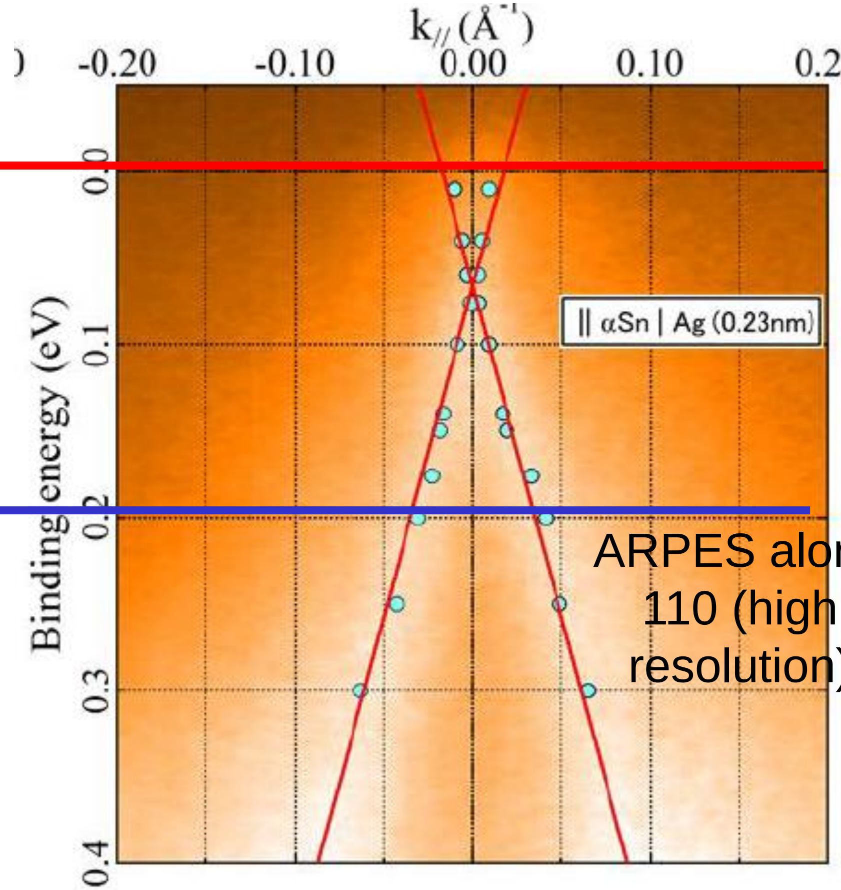

ARPES along 110 (high resolution)

Rojas-Sanchez et al,
PRL 116, 096602 (2016)

Dots correspond to maximum intensity in E=cst scans

Relaxation time τ of out of equilibrium states in Rashba or TI 2DEGs

1) Ulta-fast time-resolved ARPES (ex:$Bi_{2.2}Te_3$ Hajlaoui et al, Nat. Comm. 2013)

τ in the ps range

(ballistic length in the µm range)

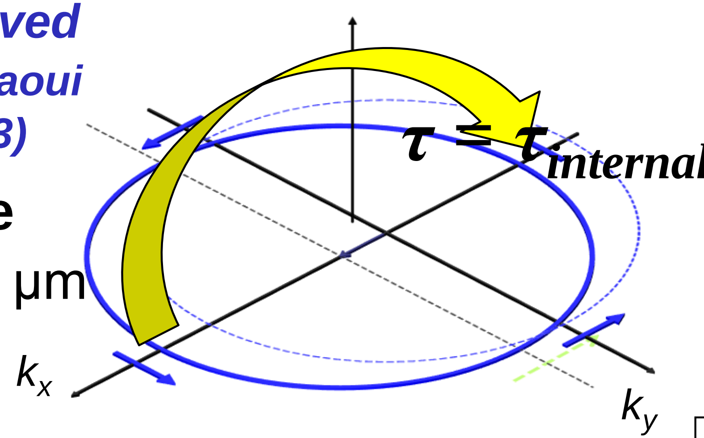

2) Spin pumping

τ in the fs range*

(ballistic lenght in the nm range)

Additional relaxation of the spin+momentum accumulation by spin-flip scattering from 2D states to 3D metal

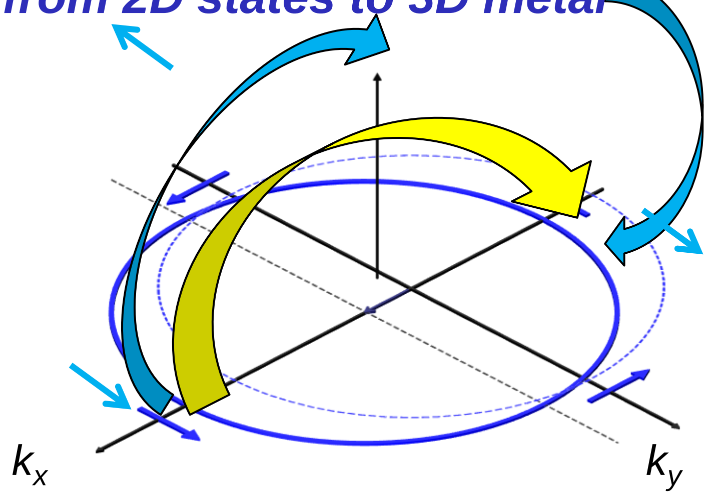

Additional relaxation by spin-flip scattering from 2DEG to metal

IEE (or EE) would more efficient (λ_{IEE} longer) without proximity of the Rashba or TI states with a metal, i.e with interface with an insulating ferromagnet (YIG, etc) or a tunnel interface

**The fs range is also the typical lifetime of QW states at the Fe/Ag interface QW, Ogawa et al, PRL 88*

LAO/STO system : large Ic production and gate effect

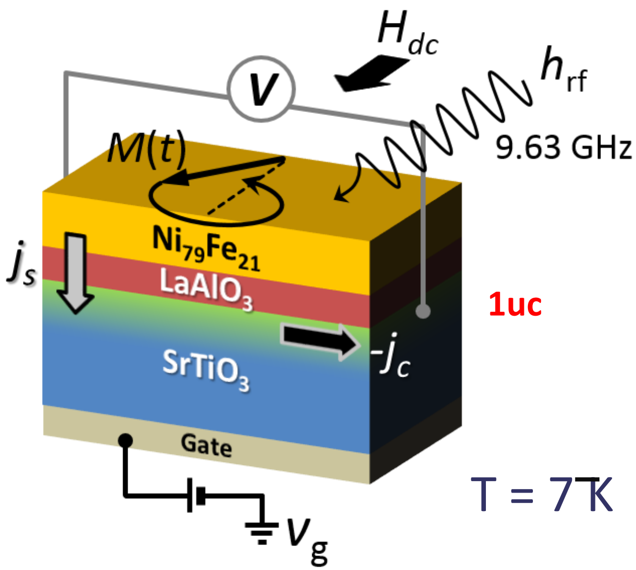

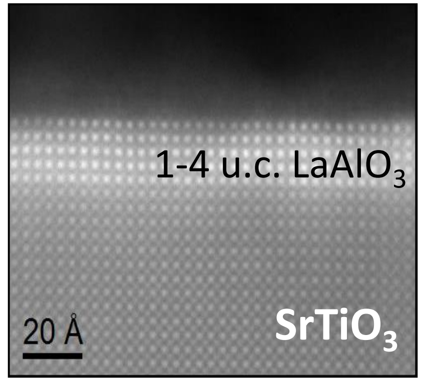

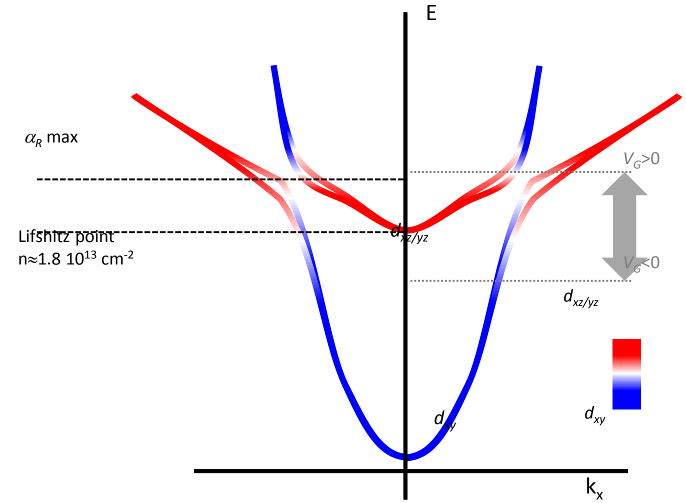

Cylindrical cavity (INAC/CEA-Grenoble) allow for measurements down to few Kelvins, combined with voltage/current probe.

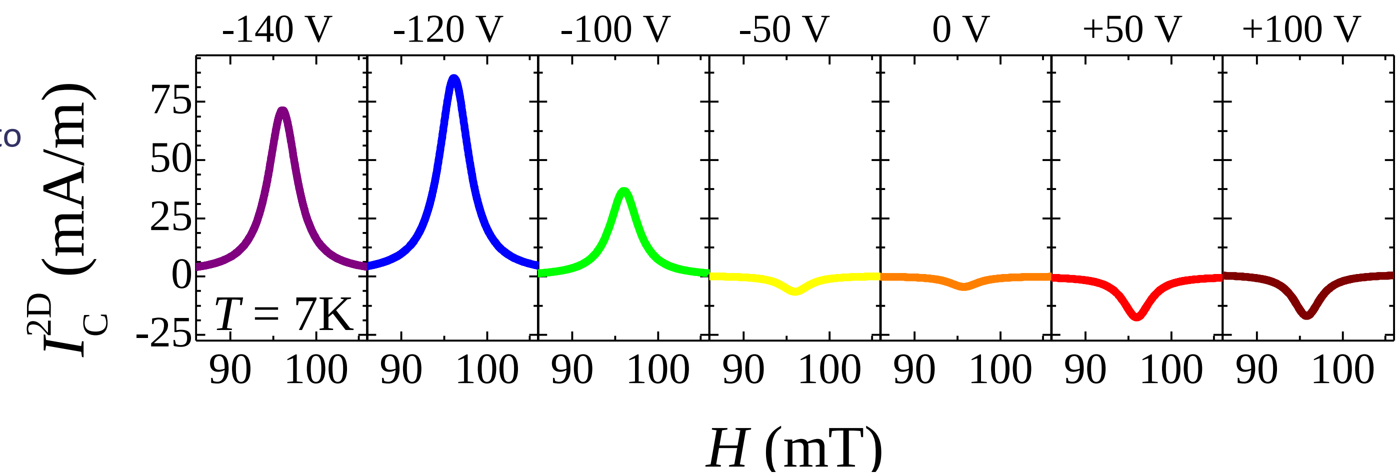

λ_{IEE} up to 6.4 nm

(definitely higher than with α-Sn and at Bi/Ag interfaces)

E. Lesne, Ph.D. Thesis,
CNRS/Thales lab.

Perspective for exploiting the conversion between spin and charge by TI in low-power spintronic devices (Room Temp.), assessment of the advantage of TI

1) **Charge to spin conversion: SHE already used in SOT-RAMS, Rashba and TI already proposed by INTEL, advantage of TI for spin-orbic logic (Manipatruni et al)**

Ex: 3-terminal SOT MRAM

Z. Wang, W. S. Zhao et al., Journal of Physics: D (2015)

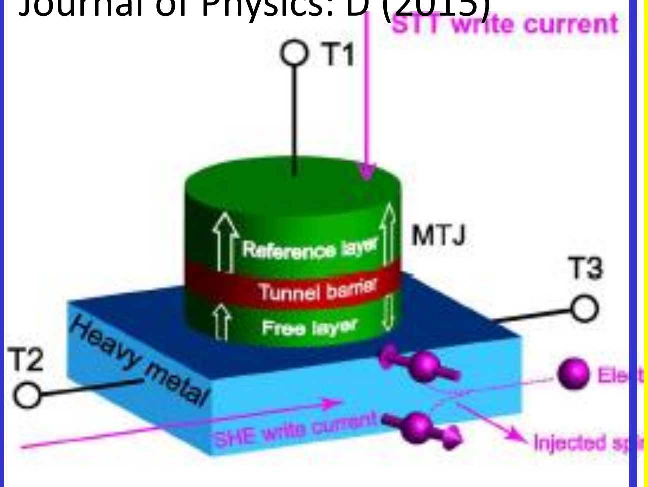

Manipatruni et al, ArXiv (Intel)

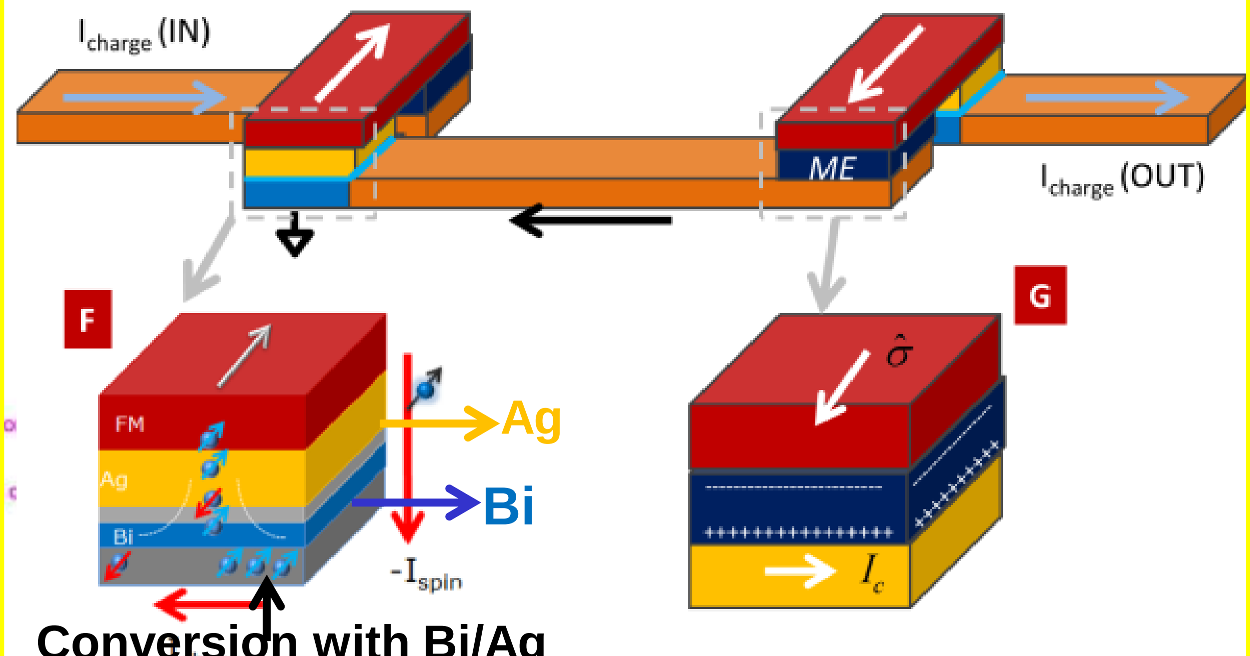

Conversion with Bi/Ag

Perspective for exploiting the conversion between spin and charge by TI in low-power spintronic devices (Room Temp.), assessment of the advantage of TI

2) **Perspective for spin to charge conversion with TI,**

first exemple: spin battery,

Microwave-driven ferromagnet–topological-insulator heterostructures: The prospect for giant spin battery effect and quantized charge pump devices

Farzad Mahfouzi,[1] Branislav K. Nikolić,[1,2] Son-Hsien Chen,[1,2,*] and Ching-Ray Chang[2,†]

[1] *Department of Physics and Astronomy, University of Delaware, Newark, DE 19716-2570, USA*
[2] *Department of Physics, National Taiwan University, Taipei 10617, Taiwan*

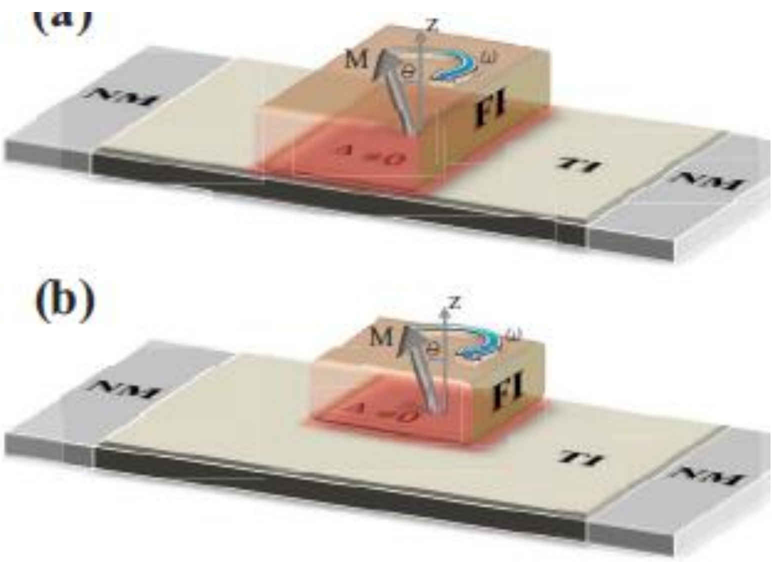

FIG. 1: (Color online) The proposed heterostructures consist of a 2D topological insulator (TI) attached to two normal metal (NM) electrodes where the ferromagnetic insulator (FI) with precessing magnetization (with cone angle θ) under the FMR conditions induces via the proximity effect a time-dependent exchange field $\Delta \neq 0$ in the TI region underneath. In the absence of any applied bias voltage, these devices pump pure spin current into the NM electrodes in setup (a) or both charge and spin current in setup (b).

Perspective for exploiting the conversion between spin and charge by TI in low-power spintronic devices (Room Temp.), assessment of the advantage of TI

2) **Perspective for spin to charge conversion with TI,**

second exemple: conversion of heat flow into electrical power

APPLIED PHYSICS LETTERS 104, 042402 (2014)

Spin Seebeck power generators

Adam B. Cahaya,[1] O. A. Tretiakov,[1] and Gerrit E. W. Bauer[2,3]

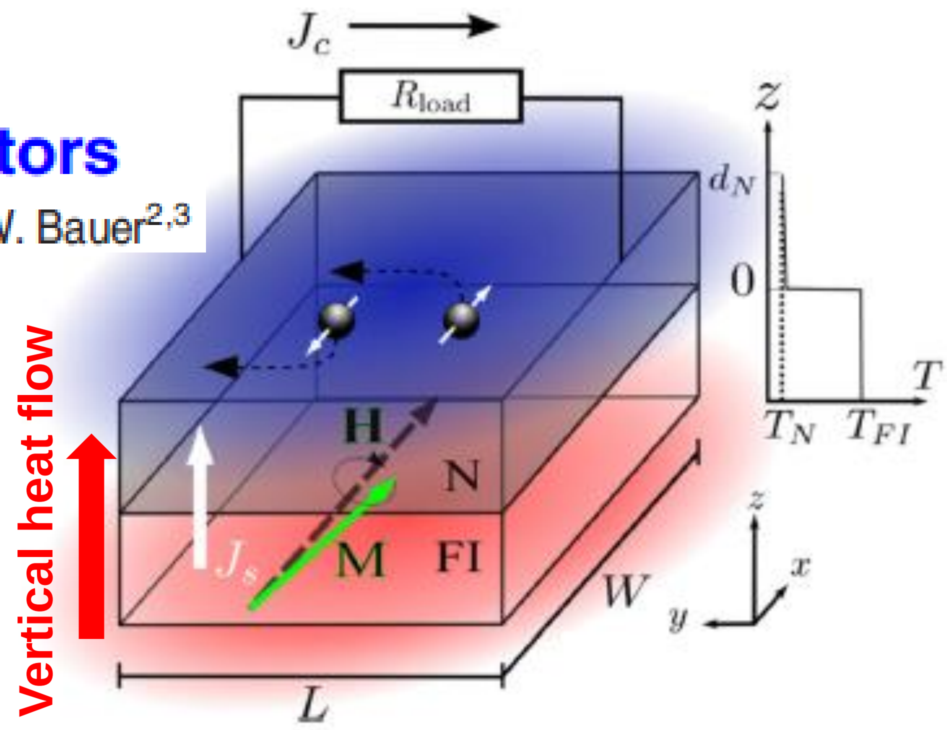

FIG. 1. A schematic view of the spin Seebeck power generator based on the ISHE. A bilayer of ferromagnetic insulator and normal metal with a low interface heat conductance pumps a spin current J_s into N. Then J_s is converted into a transverse charge current J_c by means of the ISHE.

Inverse spin Hall effect (ISHE) vs inverse Edelstein effect (IEE) WITH

3D layers

Spin-to-charge conversion by « bulk » spin-orbit effect through **inverse spin hall effect** (ISHE)

J_S^{3D}

$$ISHE: \quad \underset{(A/m^2)}{j_c^{3D}} = \Theta_{SHE} \; \underset{(A/m^2)}{j_s^{3D}}$$

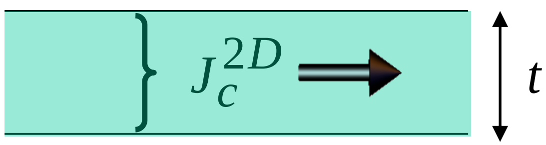

$$ISHE: J_c^{2D} = \int j_c^{3D} dz = \Theta_{SHE} l_{sf} \, th(t/2l_{sf}) \, j_s^{3D}$$

$$reaches\,its\ maximum\ J_c^{2D} = \Theta_{SHE} l_{sf} \; j_s^{3D} \ for\ t >> l_{sf}$$

$$which\ corresponds\ to\ an\ Inverse\,Edelstein\ Effect$$

$$with, at\ the\ most, an\ effective\ \lambda_{IEE}{}^{*} = \Theta_{SHE} \; l_{sf}$$

Interfaces and 2DEGs

Spin-to-charge conversion achieved through **inverse (Rashba-) Edelstein effect** (IEE)

J_S^{3D}

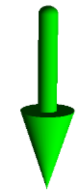

$$IEE: \quad \underset{(A/m)}{j_c^{2D}} = \lambda_{IEE} \; \underset{(A/m^2)}{j_s^{3D}}$$

Inverse spin Hall effect (ISHE) vs inverse Edelstein effect (IEE) WITH

3D layers

Spin-to-charge conversion by « bulk » spin-orbit effect through **inverse spin hall effect** (ISHE)

J_S^{3D}

$$ISHE: \quad \underset{(A/m^2)}{j_c^{3D}} = \Theta_{SHE} \; \underset{(A/m^2)}{j_s^{3D}}$$

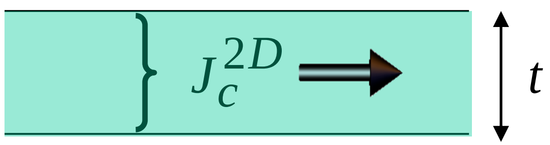

Interfaces and 2DEGs

Spin-to-charge conversion achieved through **inverse (Rashba-) Edelstein effect** (IEE)

J_S^{3D}

$$IEE: \quad \underset{(A/m)}{j_c^{2D}} = \lambda_{IEE} \; \underset{(A/m^2)}{j_s^{3D}}$$

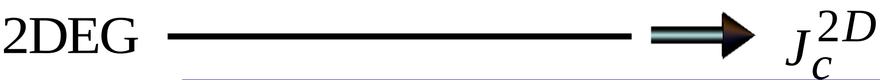

$$ISHE: J_c^{2D} = \int j_c^{3D} dz = \Theta_{SHE} l_{sf} \, th(t/2l_{sf}) \, j_s^{3D}$$

$$reaches\ its\ maximum\ J_c^{2D} = \Theta_{SHE} l_{sf} \; j_s^{3D} \ for\ t >> l_{sf}$$

which corresponds to an Inverse Edelstein Effect

with, at the most, an effective $\lambda_{IEE}^{*} = \Theta_{SHE} \, l_{sf}$

Maximum charge current induced by ISHE characterized by the effective conversion length

$$\lambda^*_{SHE} = \theta_{SHE} l_{sf}$$

to be compared to

$$\lambda_{IEE}$$

from ISHE to IEE the gain in current is at least $\lambda_{IEE} / \lambda^*_{SHE}$

Compared spin to charge conversion yield of TI (α-Sn) and ISHE (Pt and W)

1) Gain in charge current J_C for the same injected spin current density j_S from SHE in Pt or W (for t >> l_{sf}) to α-Sn (taken as an example of TI, λ=2.1nm)

- Gain from **Pt** (θ_{SHE}= 0.056*, l_{sf} = 3.4nm*) to **α-Sn**: J_C(α-Sn)/J_C(Pt) =11.03

(Pt would be as efficient as α-Sn if its SH-angle was 62%instead of 5.6%)

- Gain from **W**(θ_{SHE} = 0.33**, l_{sf} = 1.4nm***) to **α-Sn**: J_C(α-Sn)/ J_C(W) = 4.5

or from **W** with θ_{SHE} = 0.19***, l_{sf} = 1.4nm*** to **α-Sn**: J_C(α-Sn)/ J_C(Pt) = 7.9

(W would be as efficient as α-Sn if its SH-angle was 150% instead of 19-33%)

* from *C.Rojas-Sanchez et al,PRL112, 2014*

** *from Pai et al, APL 101, 2012*

*** *from Kim et al, arXiv:150308903 2*

Compared spin to charge conversion yield of TI (α-Sn) and ISHE (Pt and W)

2) Gain in electrical power P_C for the same injected spin current density ,

with $P_C = R_{\square} \mathbf{J_C}^2$

Optimal condition: $R_{\square} \simeq 4\mathrm{k}\Omega$ for α-Sn surface 2DEG between insulating materials

and $R_{\square} = \rho/t$ for the SHE metal layer (Pt, W) of optimal t = l_{sf})

- Gain from **Pt** (θ_{SHE}= 0.056, l_{sf} = 3.4nm, resistivity = 17 μΩcm) to **α-Sn**

P_C(α-Sn)/ P_C(Pt) ~ $\mathbf{10^4}$

-Gain from **W** (θ_{SHE} = 0.19-33, l_{sf} = 1.4nm, resistivity =160 μΩcm)) to **α-Sn**

P_C(α-Sn)/ P_C(W) ~ $\mathbf{10^3}$

Compared **charge to spin (or charge to torque)** conversion yields between

1) **TI $(Bi_{1-x}Sb_x)Te_3$**

with conversion factor $\mathbf{j_S/J_C \equiv q_{ICS} \simeq 1nm^{-1}}$

(Kondou et al, ArXiv:1510.03572)

and

2) **SHE-Pt or - W** layers with $\mathbf{j_S/J_C = \theta_{SHE}/l_{sf}}$

in the optimal conditions $t = l_{sf}$

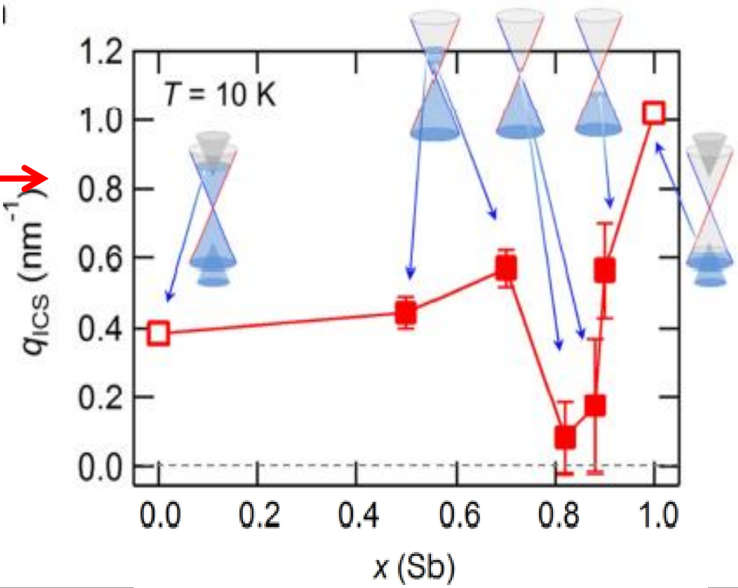

1) Gain in ejected 3D spin current density $\mathbf{J_S}$ for the same 2D charge current density $\mathbf{j_C}$ in metal layer or 2D topological states between **SHE with Pt or W (for $t \simeq l_{sf}$)** and **$(Bi_{1-x}Sb_x)Te_3$** ($q_{ICS} \simeq 1nm^{-1}$)

- Gain from Pt (θ_{SHE} = 0.056, l_{sf} = 3.4nm) to α-Sn: j_S(BiSbTe)/ j_S(Pt) = 61
- Gain from W (θ_{SHE} = 0.33, l_{sf} = 1.4nm) to α-Sn: j_S(BiSbTe)/ j_S(Pt) = 4.2

or with θ_{SHE} = 0.19, l_{sf} = 1.4nm: j_S(BiSbTe)/ j_S(Pt) = 7.4

Compared **charge to spin** conversion yields between

1) **TI $(Bi_{1-x}Sb_x)Te_3$**

with conversion factor $\mathbf{j_S/J_C \equiv q_{ICS} \simeq 1nm^{-1}}$

(Kondou et al, ArXiv:1510.03572)

and

2) **SHE-Pt or - W** layers with $\mathbf{j_S/J_C = \Theta_{SHE}/l_{sf}}$

in the optimal conditions $t = l_{sf}$

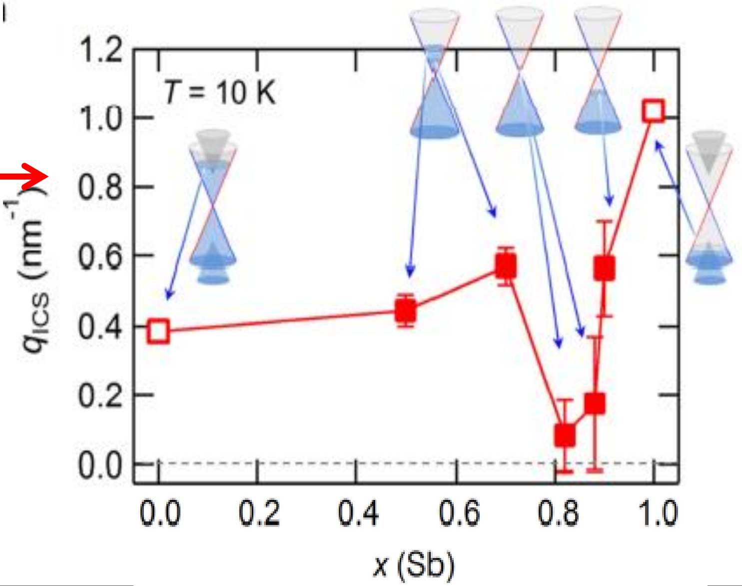

1) Gain in ejected 3D spin current density $\mathbf{J_S}$ for the same 2D charge current density $\mathbf{j_C}$ in metal layer or 2D topological states between **SHE with Pt or W (for $t \simeq l_{sf}$)** and **$(Bi_{1-x}Sb_x)Te_3$ ($q_{ICS} \simeq 1nm^{-1}$)**

- Gain from Pt ($\theta_{SHE} = 0.056$, $l_{sf} = 3.4$nm) to α-Sn: j_S(BiSbTe)/ j_S(Pt) = 61
- Gain from W ($\theta_{SHE} = 0.33$, $l_{sf} = 1.4$nm) to α-Sn: j_S(BiSbTe)/ j_S(Pt) = 4.2

or with $\theta_{SHE} = 0.19$, $l_{sf} = 1.4$nm: j_S(BiSbTe)/ j_S(Pt) = 7.4

Remark: simple calculations lead to $\mathbf{q_{ICS} = 1/v_F\tau}$ and $\mathbf{\lambda_{IEE} = 1/v_F\tau = v_F\tau}$ but τ **has not exactly the same meaning in q_{ICS}** and λ_{IEE}

Summary

Spin-charge conversion in spintronics

-Spin-Orbit in 2D system (Rashba, TI, LAO/STO) more efficient than in 3D (SHE) for spin-charge conversion

- TI can work at RT (as well as Rashba interfaces)

- TI more efficient if topological 2DEG protected by interface with insulator (ex: LAO/STO)

- Other TI-based devices: spin-filtering p-n junctions, high-speed opto-spintronics, thermo-

Thanks to all my coworkers

K. Garcia , J-M. George, H.Jaffres, N. Reyren, **J-C Rojas-Sánchez**, CNRS/Thales

L. Vila, J.-P. Attané, G. Desfond, Y. Fu, S. Gambarelli, M. Jamet, A. Marty, S. Oyarzun,. L. Vila, CEA Grenoble

J.M. De Teresa, Un. Zaragoza, Y. Ohtsubo, A. Taleb, SOLEIL Synchrotron

C.Rinaldi, M.Cantoni, R.Bertacco, Milano, R.Wang, R.Calarco, Berlin (Drude)

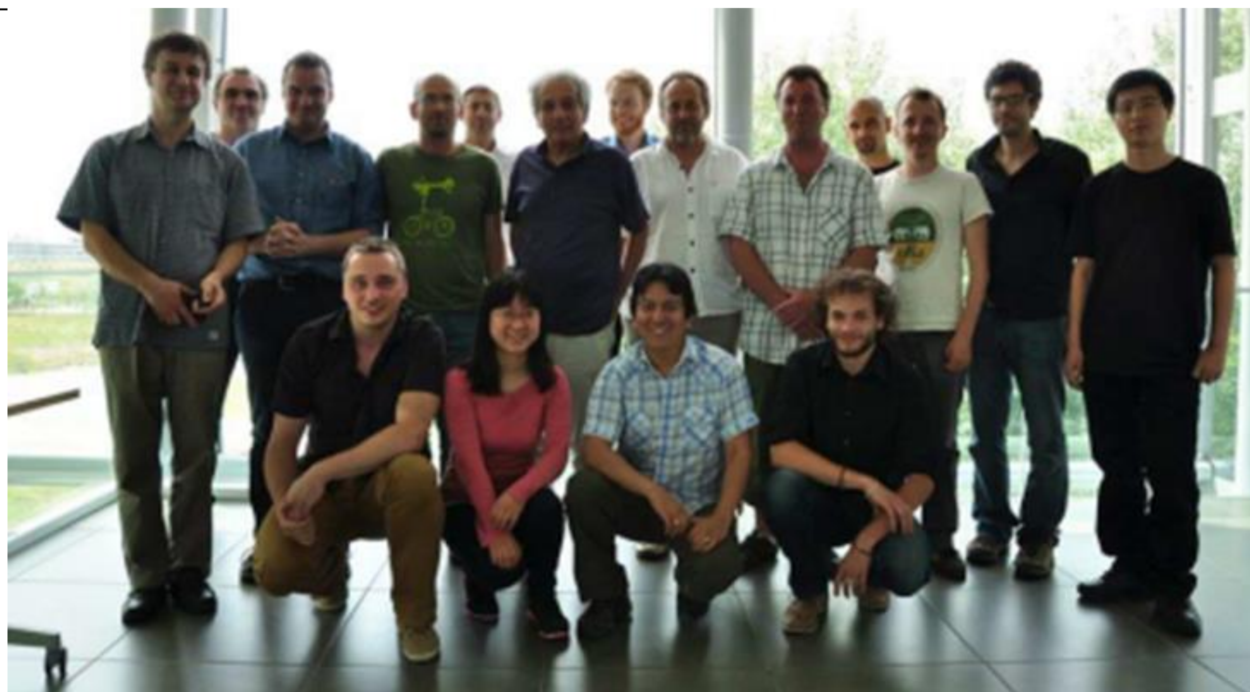

Agence Nationale de la Recherche ANR

SPINHALL + SOSPIN

Spin pumping from FMR

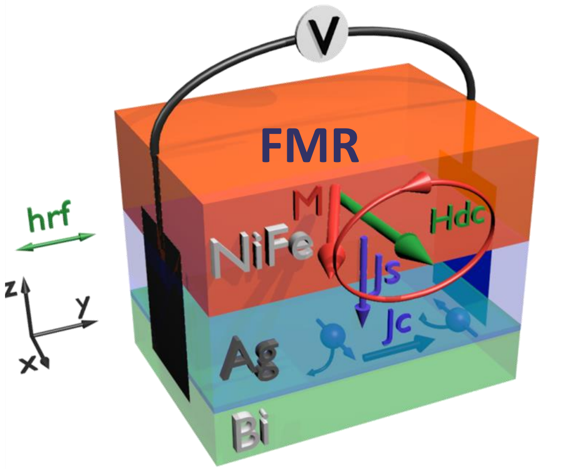

Spin pumping : generation of out of equilibrium spin distribution in FM and spin current injection in adjacent layer

Tserkovnyak et al. PRL 88, 117601 (2002)

1) Increase of effective damping and FMR linewidth

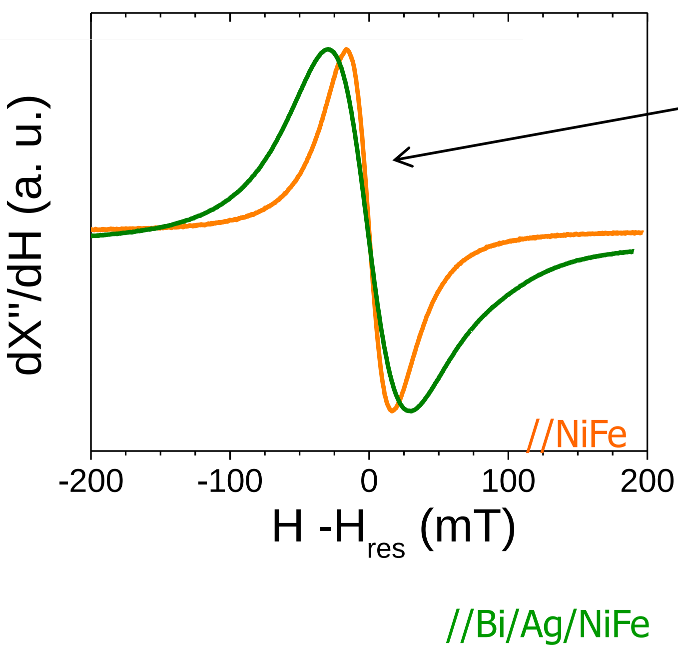

$$\alpha_{FM/NM} - \alpha_{FM} = \frac{g\mu_B}{4\pi M_s t_F} g_{eff}^{\uparrow\downarrow} \quad (1)$$

Y. Tserkovnyak et al. RMP 77, 1375 (2005)

2) Injected spin current from $g^{\uparrow\downarrow}$ derived from $\Delta\alpha$

$$J_{s0}^{int} = \frac{g_{eff}^{\uparrow\downarrow}\gamma^2\hbar h_{rf}^2}{8\pi\alpha^2}\left[\frac{4\pi M_s\gamma + \sqrt{(4\pi M_s\gamma)^2 + 4\omega^2}}{(4\pi M_s\gamma)^2 + 4\omega^2}\right] \quad (2)$$

K. Ando, E. Saitoh et al. JAP 108 , 113925 (2010)

etc

PHYSICAL REVIEW B **90**, 125312 (2014)

Topological α-Sn surface states versus film thickness and strain

S. Küfner,* M. Fitzner, and F. Bechstedt

Institut für Festkörpertheorie und -optik, Friedrich-Schiller-Universität Jena, Max-Wien-Platz 1, 07743 Jena, Germany

The theoretical prediction that gray tin represents a strong topological insulator under strain [L. Fu and C.L. Kane, Phys. Rev. B **76**, 045302 (2007)] is proven for biaxially strained α-Sn layers with varying thickness by means of a generalized density functional theory with a nonlocal exchange-correlation potential that widely simulates quasiparticle bands and a tight-binding method including intra- and interatomic spin-orbit interaction.

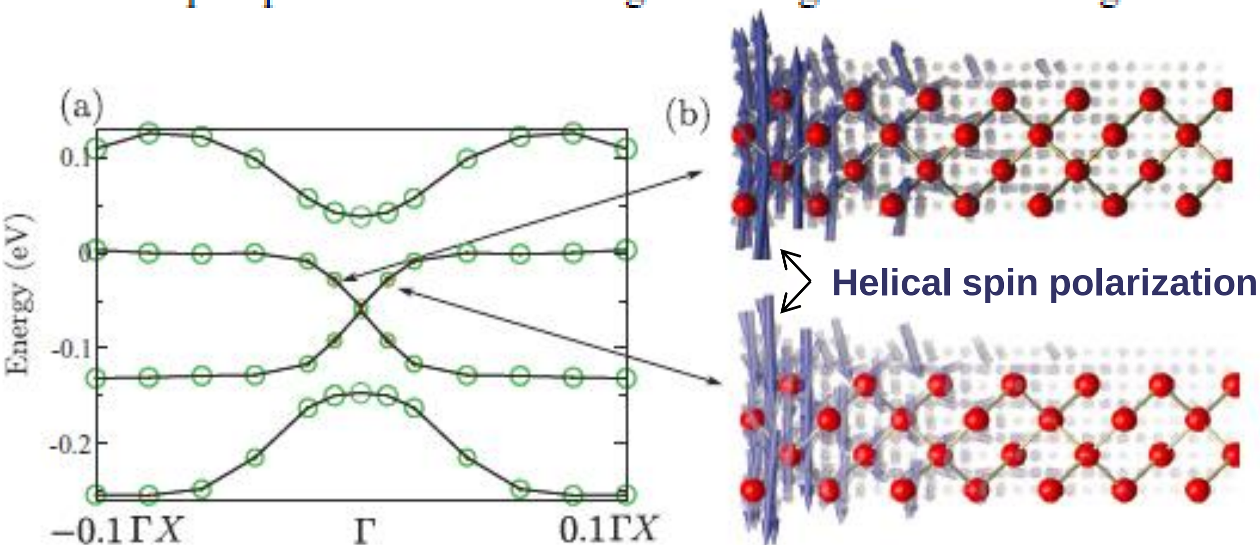

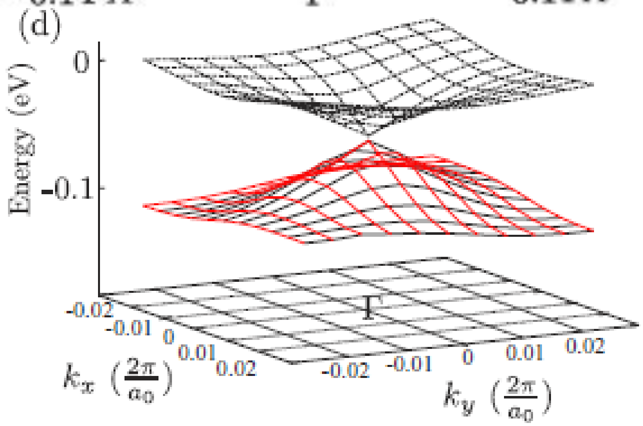

DFT-LDA for 44 ML of 0.23% biaxially strained α-Sn(001)

PHYSICAL REVIEW B **90**, 125312 (2014)

Topological α-Sn surface states versus film thickness and strain

S. Küfner,* M. Fitzner, and F. Bechstedt

Institut für Festkörpertheorie und -optik, Friedrich-Schiller-Universität Jena, Max-Wien-Platz 1, 07743 Jena, Germany

The theoretical prediction that gray tin represents a strong topological insulator under strain [L. Fu and C.L. Kane, Phys. Rev. B 76, 045302 (2007)] is proven for biaxially strained α-Sn layers with varying thickness by means of a generalized density functional theory with a nonlocal exchange-correlation potential that widely simulates quasiparticle bands and a tight-binding method including intra- and interatomic spin-orbit interaction.

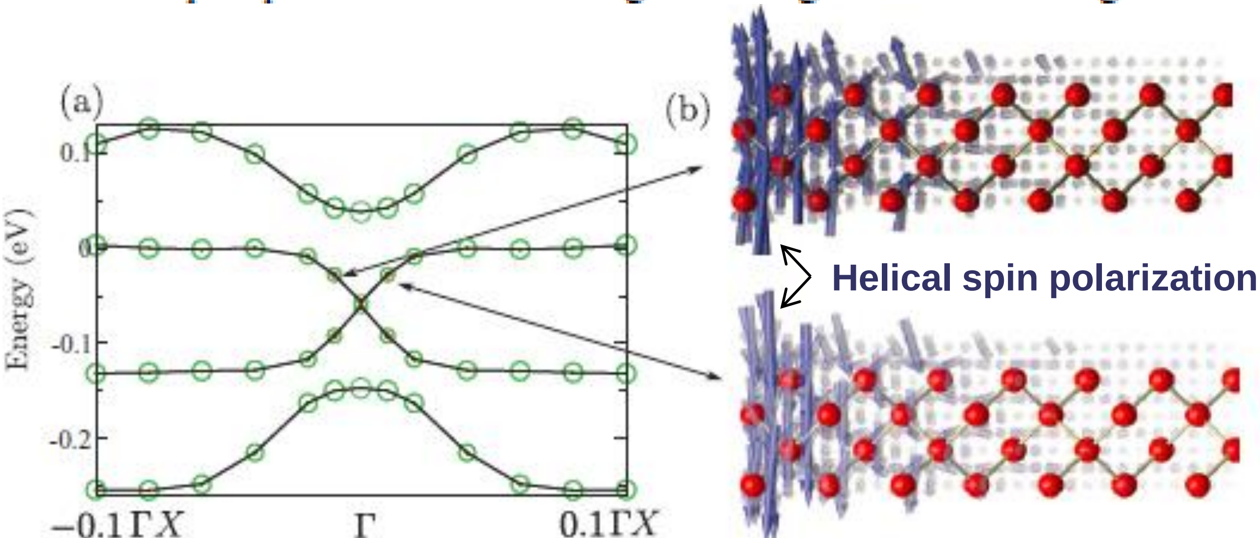

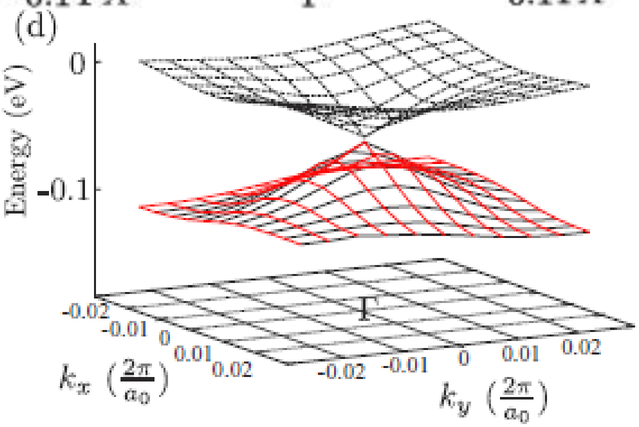

DFT-LDA for 44 ML of 0.23% biaxially strained α-Sn(001)

They are localized near the slab surfaces. Apart from atomic oscillations in Fig. 2(c) the envelope shows a localization near the surface and an exponential decay into the bulk region of the slab with a decay constant of about 10.1 A° . As consequence the overlap of envelope functions belonging to opposite surfaces of the slab with 40 ML is negligibly small.

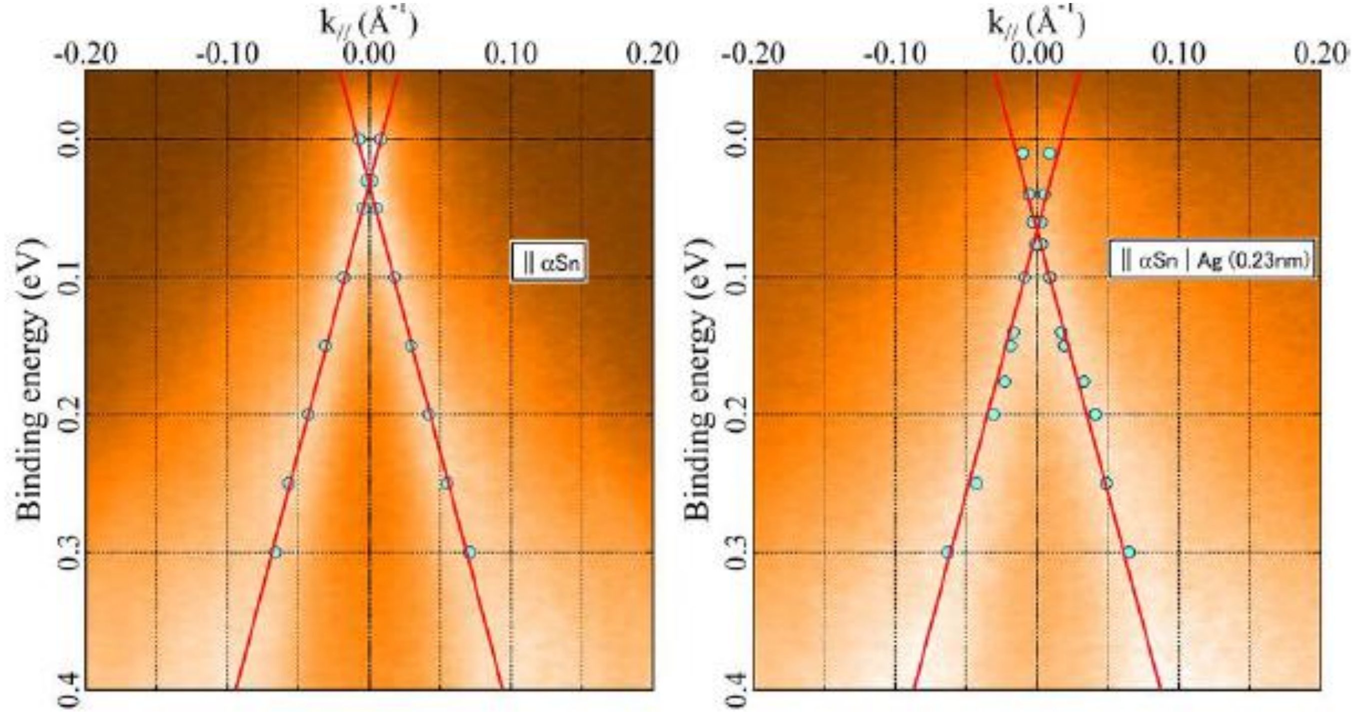
k// (Å⁻¹)
-0.20
-0.10
0.00
0.10
0.20
Binding energy (eV)
0.0
0.1
0.2
0.3
0.4
|| αSn
|| αSn | Ag (0.23nm)

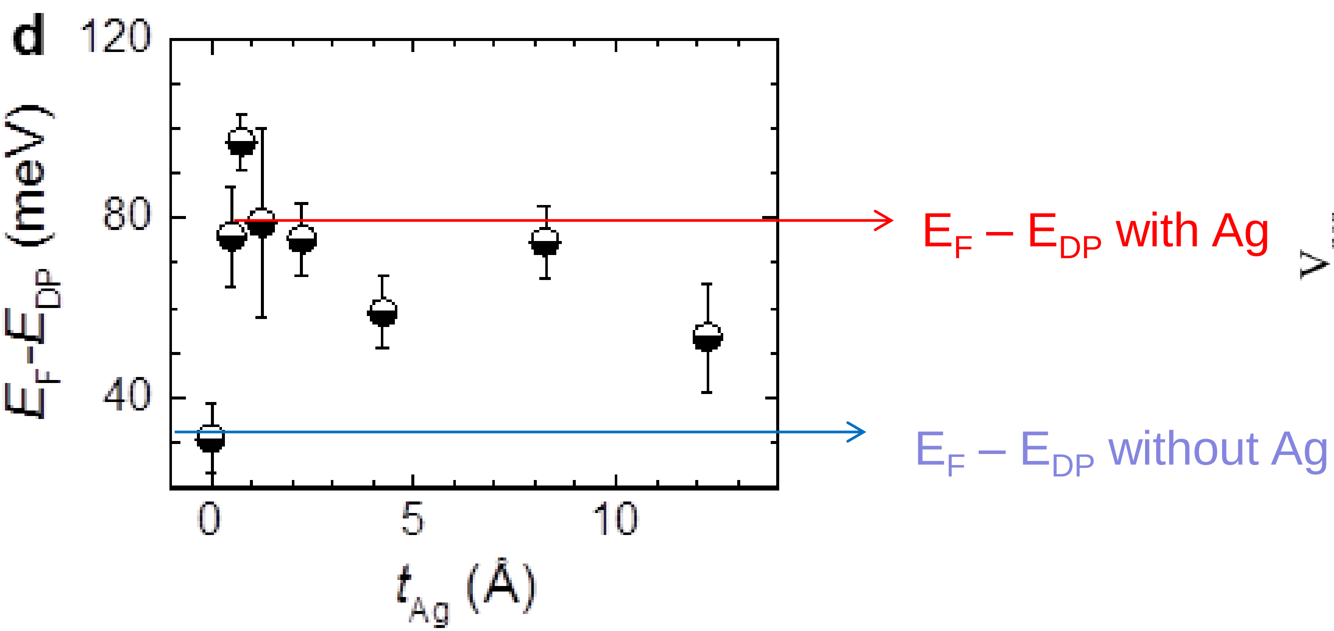
d
120
80
40
E_F-E_{DP} (meV)
0
5
10
t_{Ag} (Å)
E_F – E_{DP} with Ag
E_F – E_{DP} without Ag

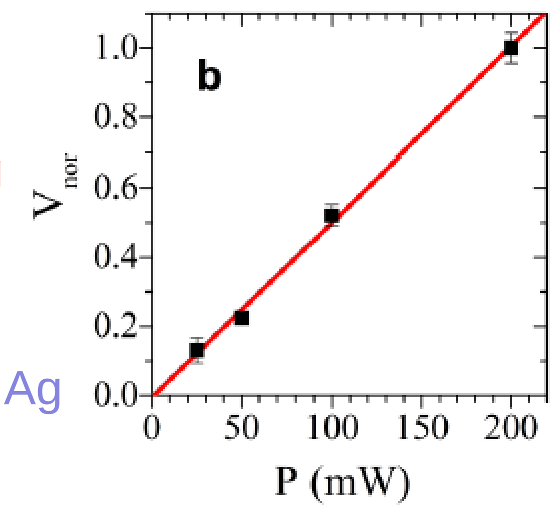
b
V_{nor}
0.0
0.2
0.4
0.6
0.8
1.0
0
50
100
150
200
P (mW)